JACS
JOURNAL OF THE AMERICAN CHEMICAL SOCIETY
Article
pubs.acs.org/JACS

Catalytic Trimerization of Bis-silylated Diazomethane

Muhammad Farooq Ibad,[†,‡] Peter Langer,[‡,§] Fabian Reiß,[†] Axel Schulz,*[,†,§] and Alexander Villinger*[,†]

[†]Abteilung Anorganische Chemie and [‡]Abteilung Organische Chemie, Institut für Chemie, Universität Rostock, Albert-Einstein-Straße 3a, D-18059 Rostock, Germany

[§]Leibniz-Institut für Katalyse e.V. an der Universität Rostock, Albert-Einstein-Straße 29a, D-18059 Rostock, Germany

Supporting Information

ABSTRACT: $(Me_3Si)_2CNN$ isomerizes upon addition of traces of $[Me_3Si]^+$ ions to give $(Me_3Si)_2NNC$, which then undergoes an unusual trimerization reaction to give exclusively 4-diazenyl-3-hydrazinylpyrazole. As catalyst the isonitrilium ion, $[(Me_3Si)_2NNC(SiMe_3)]^+$, was identified and fully characterized. Experiments and computations indicate a three-step reaction including isomerization of diazomethane, a C−C or N−C coupling, and a formal cycloaddition reaction. The kinetics and thermodynamics are discussed on the basis of DFT calculations.

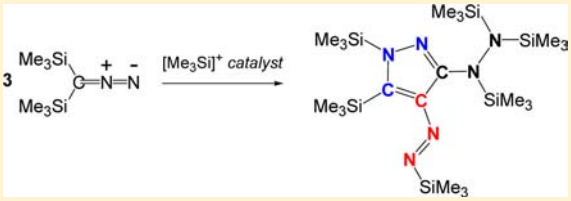

1. INTRODUCTION

More than a decade after the first isolation and characterization of silylium ions,[1] their chemistry has been an area of rapid growth,[2] since many applications have been found due to their useful properties such as enormous Lewis acidity and catalytic behavior.[3−6] For example, Ozerov et al.[4] and Müller et al.[3j] utilized silylium ions as reactive catalysts for the activation of C−F bonds. The Ozerov group introduced a class of carborane-supported, highly electrophilic silylium compounds that act as long-lived catalysts for hydro-defluorination of perfluoroalkyl groups by widely accessible silanes under mild conditions. The reactions are completely selective for aliphatic carbon−fluorine bonds in preference to aromatic carbon−fluorine bonds.[4] Recently, Oestreich et al.[3h] demonstrated that a tamed, ferrocene-based silylium ion catalyzes demanding Diels−Alder reactions in an unprecedented temperature range.

Tri-coordinate silylium (also silylenium or silicenium) ions,[2,7] with their electron sextet and a vacant p orbital, are electron-deficient species and therefore strong Lewis acids. Even relatively weak Lewis bases such as π/σ-donor solvents (toluene,[8] CH_3CN,[9] etc.) form tetrahedral complexes with silylium ions.[8,10] In addition, intramolecular π coordination in silylium ions containing a 2,6-diarylphenyl scaffold was observed, which forms a Wheland-like complex.[11] The first well-documented examples of intramolecular π-stabilization in silyl cations were silanorbornyl cations.[12] The long search for a "naked" $[R_3Si]^+$ cation,[2,13] free of interactions with the environment, was finally brought to an end with the isolation and full characterization of $[(Mes)_3Si][CHB_{11}Me_5Br_6]\cdot C_6H_6$ (Mes = 2,4,6-trimethylphenyl) by the groups of Lambert and Reed in 2002.[14]

The silylium ion $[Me_3Si]^+$ might be regarded as a sterically demanding big proton,[15] and, similar to a proton, the bulky silylium ion is always solvated, forming the $[Me_3Si_{(solv)}]^+$ ion.[8b,15−18] For example, the full series of salts containing the bis-silylated halonium/pseudo-halonium cations $[Me_3Si{-}X{-}SiMe_3]^+$ (X = F, Cl, Br, I;[15] CN, N_3, OCN, SCN;[19] CF_3SO_3[20]) were generated and fully characterized using the super Lewis acidic silylating media $Me_3Si{-}X$ and $[Me_3Si_{(solv)}]^+$ salt.[15] In view of the success of the pseudo-halogen concept in super Lewis acidic silylating media,[15,19,20] we were intrigued by the idea of utilizing the enormous Lewis acidity of the $[Me_3Si]^+$ ion to activate small molecules such as bis-silylated diazomethane $(Me_3Si)_2CNN$, aminoisonitrile $(Me_3Si)_2NNC$, and carbodiimide $(Me_3Si)NCN(SiMe_3)$, which can be considered as 16-electron-containing pseudo-chalcogens.[21] In analogy to pseudo-halogens, pseudo-chalcogens are species that form a homologous series H_2Y, MYH, M_2Y, in which alkali, alkaline earth, and heavy metals are typical representatives for M, and Y = NCN, CNN, NNC, CCO, CC, etc. Furthermore, the pseudo-chalcogen group is completely integrated in the resulting mesomeric bond system, and localization of the ionic charge at the terminal atoms is observed. Pseudo-chalcogenide anions can also act as bidentate ligands and are distinguished by their ambident nature.[21] To the best of our knowledge, salts containing silylated $[(Me_3Si)_2CNN(SiMe_3)]^+$, $[(Me_3Si)_2NNC(SiMe_3)]^+$, and $[(Me_3Si)_2NCN(SiMe_3)]^+$ have not yet been reported.

In this study, special attention was given to the diazomethane compound, as it is an ambivalent reagent.[22,23] While electrophiles commonly attack at the nucleophilic C atom,[24] nucleophiles prefer the terminal N atom of diazomethane.[25] This ambivalent behavior was also observed in [3+2] cycloaddition reactions with dipolarophiles.[26] Herein, we report what is, to the best of our knowledge, the first trimerization of a bis-silylated diazomethane, which provides, based on the use of $[(Me_3Si)_2NNC(SiMe_3)]^+$ as a catalyst, an efficient and facile synthesis of 4-diazenyl-3-hydrazinyl-1*H*-pyrazoles. Pyrazoles represent one of the most important classes of heterocyclic

Received: August 15, 2012
Published: September 22, 2012

ACS Publications © 2012 American Chemical Society

dx.doi.org/10.1021/ja308104k | J. Am. Chem. Soc. 2012, 134, 17757−17768

compounds.[27] Although a great variety of substituted pyrazoles are known, only a few examples of diazenyl- or hydrazinylpyrazoles have been described in the literature so far.[28] Likewise, di(hydrazinylidene)pyrazoles have only been scarcely reported in the literature.[29] To the best of our knowledge, trimerization reactions of diazomethane compounds have not yet been described; however, dimerizations of ethyl diazoacetate[30a,b] and of a (diazomethylene)phosphorane[30c] were previously reported to yield 1,2,4,5-tetrazine derivatives. As early as 1947, Meerwein reported the catalytic decomposition of diazomethane, yielding polymethylene.[31]

2. RESULTS AND DISCUSSION

For the molecule $(Me_3Si)_2CNN$, three acyclic constitutional isomers with an NNC unit can be formulated (Scheme 1).[32]

Scheme 1. Isomerization of Bis-silylated Diazomethane Catalyzed by $[Me_3Si{-}S]^+$ with S = Isomer 1, 2, or 3[32]

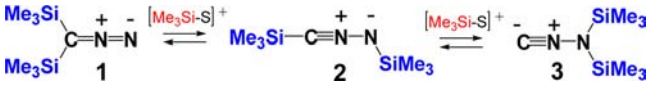

Bis(trimethylsilyl)diazomethane (**1**)[33] and bis(trimethylsilyl)-aminoisonitrile ($(Me_3Si)_2NNC$, **3**)[34] are experimentally known, but no structural data are available (Figure 1). Wiberg et al.

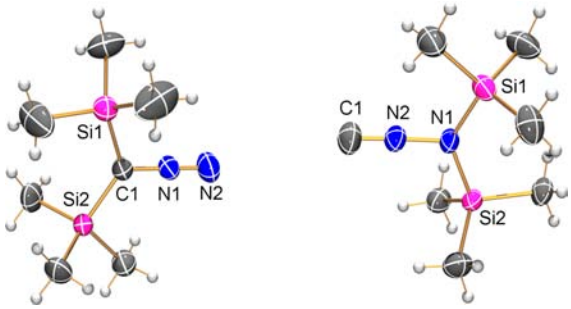

Figure 1. ORTEP drawing of the molecular structures of $(Me_3Si)_2CNN$ (left) and $(Me_3Si)_2NNC$ (right) in the crystal. Thermal ellipsoids with 50% probability at 173 K. Selected bond lengths (Å) and angles (°): for $(Me_3Si)_2CNN$, N1–N2 1.135(2), N1–C1 1.312(2), C1–N1–N2 179.6(2); for $(Me_3Si)_2NNC$, N1–N2 1.366(2), N2–C1 1.152(2), C1–N1–N2 177.7(2).

have shown that nitrilimine isomer **2** cannot be isolated since it undergoes rapid isomerization to carbodiimide **4** (Scheme 2).[34] Ever since the discovery of the first *C,N*-nitrilimines by Huisgen,[35] the development of their chemistry has been hampered because of their potential instability and the lack of suitable preparative methods. Bertrand et al. established efficient routes for preparing stable nitrilimines.[36−38] Moreover,

Scheme 2. Isomerization of Bis-silylated Carbodiimide Catalyzed by $[Me_3Si{-}S]^+$ (S = Solvent)

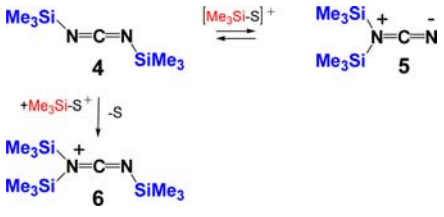

the importance of steric hindrance was shown in the stabilization of *C,N*-nitrilimines. For instance, the reaction of *n*-BuLi with $R(H)CN_2$ followed by addition of R–Cl yields the bis-silylated diazomethane R_2CNN for R = Me_3Si,[33] while the analogous reaction for the bulkier substituent R = $^iPr_3Si$ results in the formation of the thermally stable nitrilimine R–CNN–R, which only isomerizes to the carbodiimide R–NCN–R under photolytic conditions.[39]

Besides **1** and **3**, bis-silylated carbodiimde species **4** (Scheme 2)[40] was studied for comparison. **4** can be regarded as a constitutional isomer of **1**–**3** regarding the NCN unit. Only the *N,N′*-substituted carbodiimide species **4** can be isolated and structurally characterized,[40] while *N,N*-bis-silylated carbodiimde species **5** is unstable regarding the isomerization to species **4**. For the reaction with silylium ions, compounds **1**, **2**, and **4** were utilized as starting materials. All three compounds are thermally stable liquids and do not isomerize or show any other reactivity in pure form at 298 K in the dark.

2.1. Reaction of $(Me_3Si)_2CNN$, $(Me_3Si)_2NNC$, and $(Me_3Si)NCN(SiMe_3)$ with Silylium Ions and Other Strong Lewis Acids. The reaction of bis(trimethylsilyl)diazomethane $(Me_3Si)_2CNN$ with a $[Me_3Si_{(solv)}]^+$ source was studied in two series of experiments (Schemes 3 and 4). At first, the reaction

Scheme 3. Catalytic Trimerization of Bis-silylated Diazomethane[32]

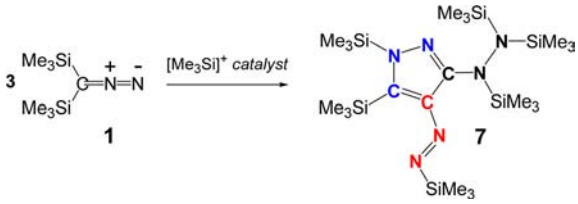

was carried out in neat $(Me_3Si)_2CNN$, generating a super Lewis acidic silylating medium. However, upon addition of $[Me_3Si_{(solv)}]^+$ salt (solv = Me_3Si–H), an immediate complex reaction contrary to the analogous reaction with Me_3Si–X (X = halogen, pseudo-halogen) was observed, resulting in a deep red, highly viscous reaction mixture. Thus *n*-pentane was added, which makes the workup and isolation of the products much easier due to a considerable decrease in the viscosity of the reaction mixture. However, it should be noted that the reaction in neat bis(trimethylsilyl)diazomethane yielded the same product. In a typical reaction setup, to a stirred suspension of $[Me_3Si_{(solv)}][B(C_6F_5)_4]$ in *n*-pentane was added a mixture of liquid $(Me_3Si)_2CNN$ (large excess) and *n*-pentane at −78 °C. The resulting suspension was allowed to warm to ambient temperature and stirred for 36 h. The reaction was followed by ^{1}H NMR experiments, and it was obvious that diazomethane $(Me_3Si)_2CNN$ was involved in a more complex chemistry under these extreme Lewis acidic conditions, beyond the simple formation of $[(Me_3Si)_2CNN(SiMe_3)]^+$ (**8**) or $[(Me_3Si)_2NNC(SiMe_3)]^+$ (**9**) (Scheme 5). Furthermore, these ^{1}H NMR experiments showed the exclusive and quantitative formation of pyrazole species **7** and the complete consumption of the starting material bis(trimethylsilyl)diazomethane (Scheme 3). The end of the reaction is indicated by deposition of the catalyst, **9**$[B(C_6F_5)_4]$, as a crystalline solid. Moreover, during the course of the reaction, the color of the supernatant changed gradually from yellow to dark red. Thus, both the precipitate and the reaction solution were further studied. The supernatant

dx.doi.org/10.1021/ja308104k | J. Am. Chem. Soc. 2012, 134, 17757−17768

Scheme 4. Catalytic Trimerization of Bis-silylated Diazomethane Utilizing $9[CHB_{11}H_5Br_6]$ as Catalyst[32]

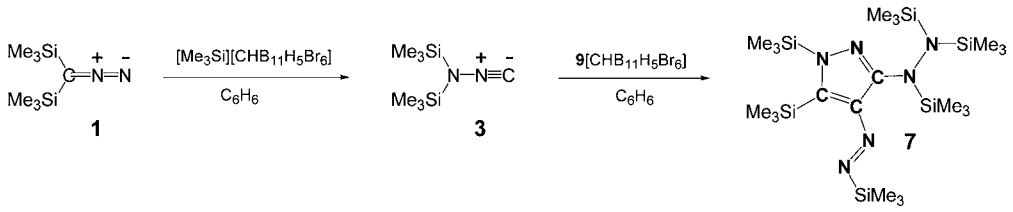

Scheme 5. Calculated Relative Gibbs Free Energies of Isomers of Neutral $(Me_3Si)_2CNN$ (1, 2, and 3) and Cationic $[(Me_3Si)_3CNN]^+$ Species (8 and 9)[a]

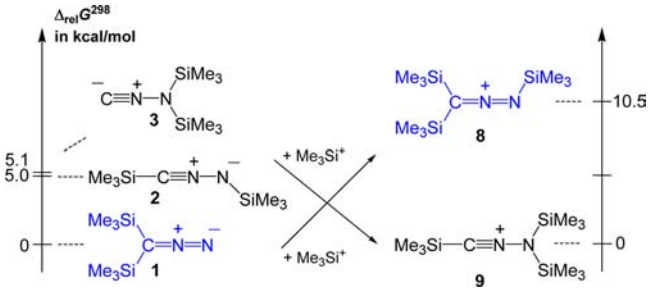

[a]Higher-lying cyclic isomers are omitted for clarity (see Supporting Information).[32]

was removed by filtration, and the brownish residue was washed with *n*-pentane. Recrystallization from a minimum of toluene at −25 °C resulted in the deposition of $9[B(C_6F_5)_4]$ as colorless crystals (49% yield based on $[Me_3Si_{(solv)}][B(C_6F_5)_4]$; Figure 2). Notably, exclusively $9[B(C_6F_5)_4]$ was isolated

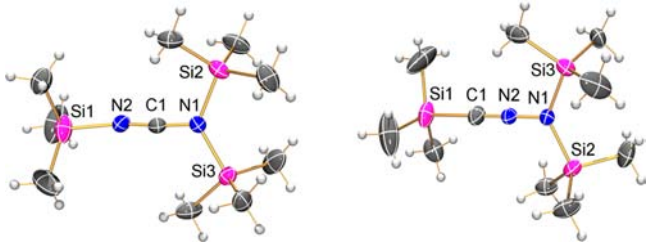

Figure 2. ORTEP drawing of the molecular structure of the $[(Me_3Si)_2NCN(SiMe_3)]^+$ ion in $6[B(C_6F_5)_4]$ (left) and the $[(Me_3Si)_2NNC(SiMe_3)]^+$ ion in $9[B(C_6F_5)_4]$ (right) in the crystal. Thermal ellipsoids with 50% probability at 173 K. Selected bond lengths (Å) and angles (°): for **6**, C1−N2 1.18(1), N1−C1 1.279 (2), N1−Si2 1.835(1), N1−Si3 1.838(1), C1−N2−Si1 159.4(9), C1−N1−Si2 115.01(8), C1−N1−Si3 116.04(8), Si2−N1−Si3 128.93(6), N1−C1−N2 173.3(5); for **9**, N1−N2 1.309(2), N2−C1 1.143(2), Si2−N1 1.818(1), Si3−N1 1.816(1), Si1−C1 1.897(2), C1−N2−N1 179.3(1), N2−N1−Si3 113.76(8), N2−N1−Si2 114.89(8), N2−C1−Si1 174.6(1), Si3−N1−Si2 131.34(6).

instead of the expected $[(Me_3Si)_2CNN(SiMe_3)][B(C_6F_5)_4]$. From the combined solutions of the filtration and washing processes, the silylated 4-diazenyl-3-hydrazinylpyrazole species (**7**) was isolated as dark green crystals (Scheme 3; see below, Figure 5 left). The overall isolated yield is about 51% (referring to $(Me_3Si)_2CNN$, which was used in a 22-fold excess both as reactant and as solvent instead of *n*-pentane) after 36 h at ambient temperatures. Referring to $[Me_3Si_{(solv)}][B(C_6F_5)_4]$), this trimerization corresponds to a catalytic process with a turnover number (TON) of about 10.8.

Since DFT calculations (see below) indicated the catalytic formation of bis(trimethylsilyl)aminoisonitrile **3** in the first reaction step (Schemes 2 and 3), in a second series of experiments isomeric **3** was reacted with $[Me_3Si_{(solv)}]^+$ under the same reaction conditions as discussed before for bis-(trimethylsilyl)diazomethane (isomer **1**). Indeed, the reaction of isomer **3** with $[Me_3Si_{(solv)}]^+$ resulted also in the exclusive formation of pyrazole species **7** along with $9[B(C_6F_5)_4]$, thus proving the computational results (see below). Since no isomerization step is needed prior to the C−C coupling and [3+2] cyclization, this reaction is faster (12 h for a complete conversion). The long-term activity and reuse of the catalyst was also studied (Table 1; see Supporting Information). Even

Table 1. Details of the Catalytic Trimerization of $(Me_3Si)_2NNC$

precatalyst[a]	mol% cat.	conversion	time/min	TON[b]
$[Me_3Si{-}H{-}SiMe_3][B(C_6F_5)_4]$	1.0	0.92	1080	92
$[Me_3Si][CHB_{11}H_5Br_5]$	2.0	0.90	180	45
$[(Et_2O)_2H][B(C_6F_5)_4]$	1.2	0.84	30	72
$[Me_3SiOEt_2][B(C_6F_5)]$	1.3	0.74	30	59
$B(C_6F_5)_3$	1.9	0.84	14400	45
$[Ph_3C][B(C_6F_5)_4]$[d]	0.9	0.89	240	100
$GaCl_3$[c]	4.9	0.00	780	0
$Ag[CHB_{11}H_5Br_5]$[c]	1.3	0.00	780	0
$[(Me_3Si)_2NCN(SiMe_3)][B(C_6F_5)_4]$	1.0	0.70	30	71

[a]Precatalyst that forms the catalyst $[LA\text{-}CNN(SiMe_3)_2]^+$ (LA = Lewis acid). [b]TON = n(NNC)×conversion/n(precatalyst). [c]No conversion to **7**, but slow decomposition to unidentified side products was observed. [d]Trityl ions do not catalyze the isomerization step.

after 14 days and several reuses, the catalyst was still active as well as when the catalyst concentration was decreased to less than 1 mol%. For instance, the reaction of aminoisonitrile **3** afforded in three runs isolated yields of pyrazole species **7** between 74 and 82% when 1 mol% catalyst was used, displaying a constant activity over all runs. A TON of 230 was estimated (36 h). After each cycle, the amount of catalyst remained almost unchanged. The catalyst can always be recovered in good yield as crystalline material at the end of the reaction.

For comparison, the reaction of carbodiimide **4** with 1 equiv of $[Me_3Si_{(solv)}][B(C_6F_5)_4]$ (solv = $Me_3Si{-}H$, toluene) dissolved in toluene leads in a straightforward, almost quantitative reaction (isolated yield 77%) to the formation of the silylated species **6** with $[B(C_6F_5)_4]^-$ as counterion (Scheme 2, Figure 2). Interestingly, no isomerization to the *N*,*N*-bis-silylated carbodiimde species **5** (Scheme 2) nor any other reactivity was observed, even under reflux conditions.

Variation of the Counteranion and the Lewis Acids. To study the influence of the anion on the trimerization process, we prepared trimethylsilylium *closo*-7,8,9,10,11,12-hexabromo-

dx.doi.org/10.1021/ja308104k | J. Am. Chem. Soc. 2012, 134, 17757−17768

carboranate $[Me_3Si][CHB_{11}H_5Br_6]$ and reacted it with (i) stoichiometrically amounts of diazomethane **1** or amino-isonitrile **3** in benzene and (ii) a large excess of **1** and **3** ($[Me_3Si][CHB_{11}H_5Br_6]$ as catalyst). As shown in Scheme 4, pyrazole species **7** was generated with the same reactivity, and it was also possible to isolate the catalytic species **9**$[CHB_{11}H_5Br_6]$ (Figure 3, Table 1).

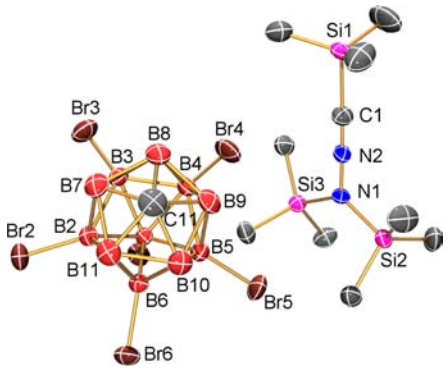

Figure 3. ORTEP drawing of the molecular structure of **9**$[CHB_{11}H_5Br_6]$ in the crystal. Thermal ellipsoids with 50% probability at 173 K. Selected bond lengths (Å) and angles (°): N1−N2 1.309(3), N2−C1 1.147(4), Si2−N1 1.816(3), Si3−N1 1.809(3), Si1−C1 1.901(3), N2−N1−Si3 115.1(2), N2−N1−Si2 115.5(2), Si3−N1−Si2,129.4(1), C1−N2−N1 178.6(4).

As listed in Table 1, in a next series of experiments several neutral ($GaCl_3$, $B(C_6F_5)_3$) and cationic Lewis acids (Ag^+, $[(Me_3Si)_2NCN(SiMe_3)]^+$ (**6**), $[Ph_3C]^+$, $[Me_3SiOEt_2]^+$, and $[(Et_2O)_2H]^+$) were tested. Except for Ag^+ and $GaCl_3$, all other Lewis acids showed a significant reactivity and can be used for the generation of pyrazole species **7**. Interestingly, in contrast to $[Ph_3C]^+$, the neutral Lewis acid $B(C_6F_5)_3$ also catalyzes the isomerization and trimerization process; however, the rates of both processes are much slower. For both $[Ph_3C]^+$ and $B(C_6F_5)_3$, we were also able to isolate and fully characterize the catalysts $[(Me_3Si)_2NNC(CPh_3)]^+$ (**10**) and $[(Me_3Si)_2NNC(B(C_6F_5)_3)]^+$ (**11**), respectively (Figure 4).

2.2. Properties and Spectroscopic Characterization. All experimentally studied compounds (**6**$[B(C_6F_5)_4]$, **9**$[B(C_6F_5)_4]$, **9**$[CHB_{11}H_5Br_6]$, **10**, and **11** as well as pyrazole species **7** and **12**) are easily prepared in large scale and are stable when stored in a sealed tube and kept at ambient temperature. All these compounds have been fully characterized. All salts are extremely air- and moisture-sensitive but stable under argon atmosphere over a long period as a solid. Toluene is a good solvent for all species; however, the three salts **6**$[B(C_6F_5)_4]$, **9**$[B(C_6F_5)_4]$, and **9**$[CHB_{11}H_5Br_6]$ are poorly soluble in non-aromatic organic solvents such as *n*-hexane or slowly decompose in, e.g., CH_2Cl_2, in contrast to neutral **10** and **11**. The $[B(C_6F_5)_4]^-$ salts of **6** and **9** melt at 104 and 108 °C, respectively, while for **9**$[CHB_{11}H_5Br_6]$ (206 °C) and **10** (136 °C) only decomposition is observed. The highest melting point is found for the neutral compound **11**, at 122 °C (Table 2).

The IR and Raman data of all isonitrile species show a sharp band in the expected region[33,41] between 2209 and 2302 cm^{-1}, which can be approximately assigned to the stretching frequency ν_{CN} (cf. 2041 cm^{-1} (IR) in $(Me_3Si)_2CNN$ and 2102 cm^{-1} (Raman) in $(Me_3Si)_2NNC$)). It should be noted that the entire CNN moiety vibrates in an asymmetric mode; however, to a good approximation the small movement of the amino nitrogen can be neglected. As previously shown, the coordination of $B(C_6F_5)_3$ to a R−CN species causes a significant band shift to higher wave numbers; thus, for the $B(C_6F_5)_3$ adduct **11**, a shift of $\Delta\nu$ = 197 cm^{-1} was observed.[42] A shift with a similar magnitude was also observed for all salts containing cation **9** (Table 2). Hence, both IR and Raman spectroscopy are particularly well suited to distinguish between the starting material **3** and the silylated cation **9**. The shift to higher wave numbers upon adduct formation correlates nicely with a smaller C−N distance (**3**, *d*(CN) = 1.152(2) Å vs **9**$[B(C_6F_5)_4]$, 1.143(2); **9**$[CHB_{11}H_5Br_6]$, 1.147(2); **10**, 1.145(2); and **11**, 1.145(4) Å; see X-ray structure elucidation, Table 3). Interestingly, the CN distance in neutral adduct **11** is almost the same as found in all cationic adducts **9** and **10**.

Pyrazole species **7** (Figure 5 left) is neither very air- nor moisture-sensitive, melts at 66 °C, and dissolves in almost all common organic solvents. Depending on the solvent, several solvates of **7** can be obtained, such as **7**·*n*-hexane and **7**·disiloxane (see below). Interestingly, one Me_3Si group can be selectively hydrolyzed by addition of 1 equiv of CF_3SO_3H or water/*n*-hexane to give pyrazole species **12** (Scheme 6, Figure 5 right).[43] It is interesting to note that crystals of **12** show dichroism under polarized light which results in a violet or orange appearance.

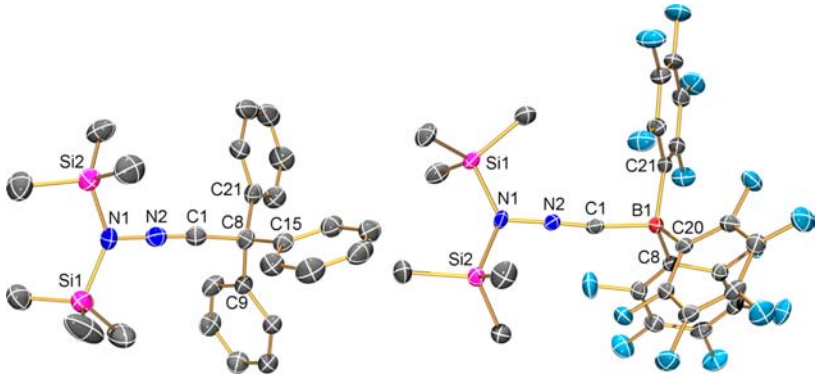

Figure 4. ORTEP drawing of the molecular structures of **10** (left) and **11** (right) in the crystal. Thermal ellipsoids with 50% probability at 173 K. Selected bond lengths (Å) and angles (°): for **10**, N2−C1 1.145(4), N2−N1 1.334(4), C1−C8 1.480(4), N1−Si2 1.818(3), N1−Si1 1.823(3), C1−N2−N1 179.1(3), N2−N1−Si2 111.9(2), N2−N1−Si1 113.3(2), Si2−N1−Si1 132.6(2); for **11**, N2−C1 1.145(2), N2−N1 1.331(2), N1−Si1 1.805(1), N1−Si2 1.805(1), C1−B1 1.617(2), C1−N2−N1 177.7(1), N2−N1−Si1 114.91(6), N2−N1−Si2 111.52(6), Si1−N1−Si2 133.35(4).

dx.doi.org/10.1021/ja308104k | J. Am. Chem. Soc. 2012, 134, 17757−17768

Table 2. Spectroscopic Details

	6[B(C$_6$F$_5$)$_4$]	9[B(C$_6$F$_5$)$_4$]	9[CHB$_{11}$H$_5$Br$_6$]	10	11
mp/°C	104	108	206[a]	136[a]	122
^{11}B NMR	−16.64[c]	−16.64[c]	−20.22 (d, 5B, *B*H), −9.84 (s, 5B, *B*Br), −1.74 (s, 1B, 12-*B*Br)	−16.64	−21.27
Ra: ν_{CN}/cm^{-1}	2251(4)	2209(9)	[b]	[b]	2299(10), 2220(3),
IR: ν_{CN}/cm^{-1}	2287(w), 2243(m)	2215(m)	2236(w), 2165(w)	2285(w)	2302(w)

[a]Decomposition temperature. [b]Strong fluorescence. [c]Slow decomposition in CD_2Cl_2

Table 3. Selected Bond Lengths (Å) and Angles (°) from X-ray Structure Analyses

compound[d]	X−Y	Y−Z	Z−R	XYZ
NNC(SiMe$_3$)$_2$ (**1**)	1.135(2)	1.312(2)	1.885(1)	179.6(2)
(Me$_3$Si)$_2$NNC (**3**)[b]	1.366(2)	1.152(2)	–	177.7(2)
(Me$_3$Si)$_2$NNC (**3**)[b]	1.361(2)	1.153(2)	–	178.4(2)
(Me$_3$Si)NCN(SiMe$_3$) (**4**)[c]	1.201(2)	1.194(2)	1.722(2)	176.6(2)
[(Me$_3$Si)$_2$NCN(SiMe$_3$)][B(C$_6$F$_5$)$_4$]	1.279(2)	1.18(1)	1.795(11)	173.3(5)
[(Me$_3$Si)$_2$NNC(SiMe$_3$)][B(C$_6$F$_5$)$_4$]	1.309(2)	1.143(2)	1.897(2)	179.3(1)
[(Me$_3$Si)$_2$NNC(SiMe$_3$)][CHB$_{11}$H$_5$Br$_6$]	1.309(3)	1.147(4)	1.901(3)	178.6(4)
(Me$_3$Si)$_2$NNC(B(C$_6$F$_5$)$_3$) (**11**)[a]	1.331(2)	1.145(2)	1.617(2)	177.7(1)
(Me$_3$Si)$_2$NNC(B(C$_6$F$_5$)$_3$) (**11**)[a]	1.342(2)	1.143(2)	1.615(2)	177.7(2)
[(Me$_3$Si)$_2$NNC(CPh$_3$)][B(C$_6$F$_5$)$_4$] (**10**)	1.334(4)	1.145(4)	1.480(4)	179.1(3)

[a]Two slightly different data sets were obtained from different experiments. [b]Two independent molecules in the unit cell. [c]See ref 44. [d]All compounds can formally be written as R′X−Y−Z−R; e.g., for **1** and **3**, X = N, Y = N, Z = C; for **4**, X = N, Y = C, Z = N, etc.

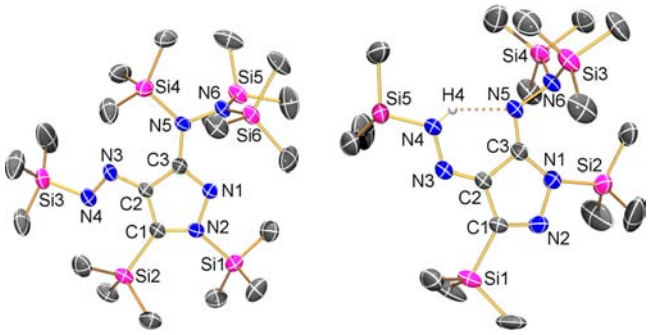

Figure 5. ORTEP drawing of the molecular structures of pyrazole species **7** (left) and **12** (right) in the crystal. Thermal ellipsoids with 50% probability at 173 K. Except from H4, all other hydrogen atoms are omitted for clarity. Selected bond lengths (Å): for **7**, N1−C3 1.324(3), N1−N2 1.400(2), N2−C1 1.355(2), N3−N4 1.272(2), N3−C2 1.389(3), N5−C3 1.387(2), N5−N6 1.455(2), C1−C2 1.398(3), C2−C3 1.425(3); for **12**, N1−C3 1.381(3), N1−N2 1.433(3), N2−C1 1.314(3), N3−C2 1.310(3), N3−N4 1.348(3), N5−C3 1.307(3), N5−N6 1.467(3), C1−C2 1.437(3), C2−C3 1.470(3).

2.3. X-ray Structural Analysis. As far as we know, there are no structural data available for the starting materials **1** and **3**, while the structures of bis-silylated carbodiimide **4** and its tetramer were reported in 1994 by Riedel et al.[44] The structures of silylium cation-containing species **6**[B(C$_6$F$_5$)$_4$], **9**[B(C$_6$F$_5$)$_4$], and **9**[CHB$_{11}$H$_5$Br$_6$], as well as **10** and **11**, besides pyrazoles **7** and **12**, were determined. Tables S1−S4 (see Supporting Information) present the X-ray crystallographic data. X-ray-quality crystals of all considered species were selected in Fomblin YR-1800 (Alfa Aesar) at ambient temperature. All samples were cooled to −100(2) °C during the measurement. The molecular structures are shown in Figures 1−5, along with selected bond lengths and angles. More details are found in the Supporting Information, including the data for the solvates **7**·*n*-hexane and **7**·disiloxane.

*Structure of the Room-Temperature Liquids (Me$_3$Si)$_2$CNN (**1**), (Me$_3$Si)$_2$NNC (**3**), and (Me$_3$Si)NCN(SiMe$_3$) (**4**).* Crystals of **1** and **3** suitable for X-ray crystallographic analysis were obtained by slow cooling of neat **1** and **3**, respectively, to −80 °C over a period of 8 h. Both species crystallized (space group for **1**, $P\bar{1}$; for **3**, *Pbca*; cf. for **4**, $P2_1/c$[44]) with two independent molecules per unit cell. Only very weak van der Waals interaction can be assumed since large distances between molecules of **1**, **3**, and **4** are observed. There are only very small differences between the structural parameters of the independent molecules. Hence only one set of data is given for **1** and **3** in Figure 1 and Table 3. In general, in both isoelectronic species **1** and **3** the NNC moiety is almost linear, with short NN and CN bond lengths displaying partial double- and triple-bond character. For diazomethane species **1** a very short NN distance, indicating triple-bond character (N1−N2 1.135(2) Å, cf. $\sum r_{cov}$(N≡N) = 1.08 Å),[45] is found, while the CN bond is much longer, at 1.312(2) Å. This situation is exactly the other way around in **3**, with a CN triple bond (1.152(2) Å, $\sum r_{cov}$(C≡N) = 1.14 Å)

Scheme 6. Selective Hydrolysis of 7

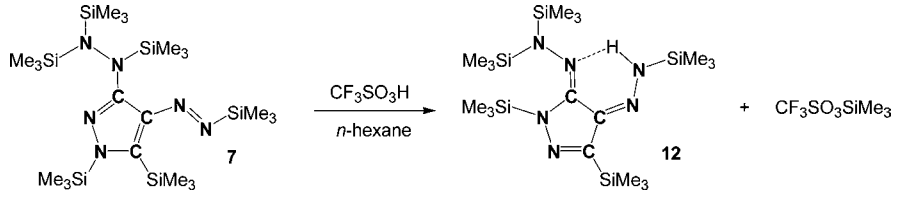

dx.doi.org/10.1021/ja308104k | J. Am. Chem. Soc. 2012, 134, 17757−17768

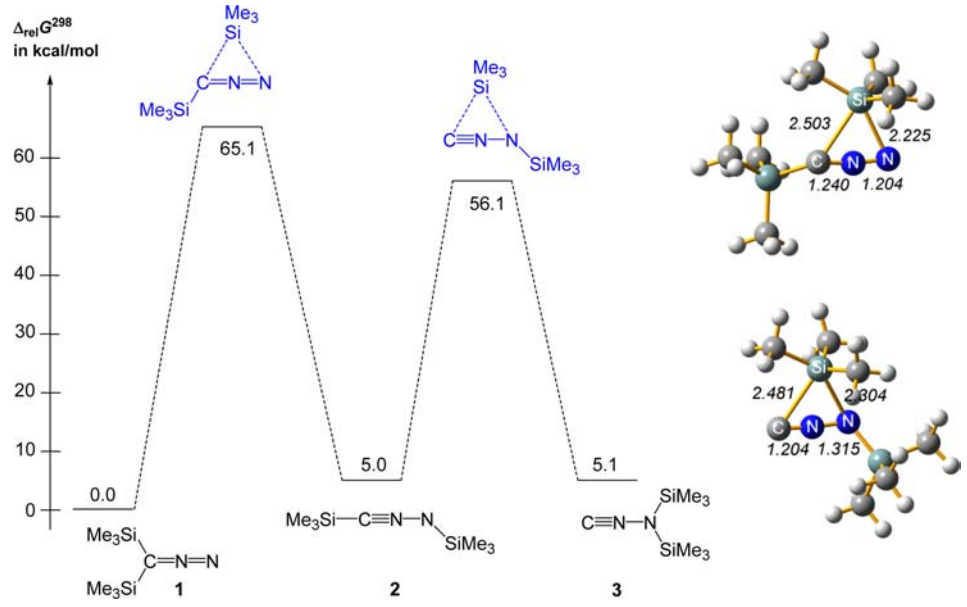

Figure 6. Left: Energies of the intrinsic isomerization process without a $[Me_3Si]^+$ ion as catalyst. Right: Calculated transition states for the intrinsic 1,3-Me_3Si shift in **1** (distances in Å).

and a rather long NN bond, at 1.366(2) Å (cf. $\sum r_{cov}$(N═N) = 1.20 Å and $\sum r_{cov}$(N−N) = 1.42 Å).[45] For comparison, in the carbodiimide species **4** the CN bond lengths amount to 1.201(2) and 1.194(2) Å, and the NCN unit is also almost linear (176.6(2)°).[44]

*[(Me$_3$Si)$_2$NCN(SiMe$_3$)][B(C$_6$F$_5$)$_4$] (**6**[B(C$_6$F$_5$)$_4$])*. The X-ray diffraction analyses (space group $P2_1/c$) revealed a disordered cation with a di-coordinated and tri-coordinated (planar) nitrogen center (sum of the angles around N1 = 360°, Figure 2 left). The strong interaction of carbodiimide with the formally added, electron-deficient $[Me_3Si]^+$ center is clearly apparent from the Si−N bond lengths (N1−Si2 1.835(1), N1−Si3 1.838(1), and N2−Si1 1.794(1) Å), which are slightly shorter than the sum of the covalent radii (1.87 Å).[45] Due to the di- and tri-coordination, respectively, two significantly different CN bond lengths (N1−C1 1.279(2), N2−C1 1.18(1) Å) are observed, in contrast to the neutral parent molecule **4** (1.201(2) and 1.194(2) Å).[44] The NCN unit is slightly bent, with 173.3(5)°, and all Si atoms are not part of the plane formed by these three atoms. Only weak interactions are found between the ions.

*[(Me$_3$Si)$_2$NNC(SiMe$_3$)][B(C$_6$F$_5$)$_4$] (**9**[B(C$_6$F$_5$)$_4$])*. Compound **9** crystallizes in the monoclinic space group $P2_1/c$ with four units per cell. As depicted in Figure 2 (right), the cation adopts a C_1-symmetric structure with an almost linear CNN unit (C1−N2−N1 179.3(1)°, cf. 179.6(2) in $(Me_3Si)_2CNN$ and 177.7(2)° in $(Me_3Si)_2NNC$, Figure 1), and a slightly bent Si1−C1−N2 angle of 174.6(1)° is found. The C−N bond length amounts to 1.143(2) Å, which nicely agrees with the sum of the covalent radii for a CN triple bond ($\sum r_{cov}$(C≡N) = 1.14 Å;[45] cf. 1.152(2) Å in $(Me_3Si)_2NNC$ or 1.157(2) Å in $[Me_3Si{-}C{\equiv}N{-}SiMe_3]^+$).[19] The N1−N2 bond is rather long, at 1.309(2) Å (cf. $\sum r_{cov}$(N═N) = 1.20 Å and $\sum r_{cov}$(N−N) = 1.42;[45] 1.135(2) Å in $(Me_3Si)_2CNN$ and 1.366(2) Å in $(Me_3Si)_2NNC$), indicating partial double-bond character. In accord with natural bond orbital analysis,[46] thus the best Lewis representation is that with a CN triple bond and an NN single bond: $[Me_3Si{-}C{\equiv}N^+{-}N(SiMe_3)_2]^+$. The tri-coordinated N1 atom sits in a trigonal planar environment ($\sum\angle$N = 360.0°) with two small N2−N1−Si angles (113.76(8) and 114.89(8)°) and one large Si3−N1−Si2 angle (131.34(6)°).

*[(Me$_3$Si)$_2$NNC(SiMe$_3$)][CHB$_{11}$H$_5$Br$_6$] (**9**[CHB$_{11}$H$_5$Br$_6$])*. As displayed in Table 3 and Figure 3, the structural parameters (bond lengths and angles) of the cation are identical (within the standard deviation) with those of **9**[B(C$_6$F$_5$)$_4$], indicating that both borate anions are true weakly coordinating anions (shortest distances between $C1_{cation}\cdots Br_{anion}$ = 3.734 Å; cf. $C1_{cation}\cdots F_{anion}$ = 3.632 Å in **9**[B(C$_6$F$_5$)$_4$]).

*[(Me$_3$Si)$_2$NNC(CPh$_3$)][B(C$_6$F$_5$)$_4$] (**10**) and [(Me$_3$Si)$_2$NNC(B(C$_6$F$_5$)$_3$)] (**11**)*. The formal change of the Lewis acid (Me_3Si^+ in **9**), as in **10** (Ph_3C^+) and **11** ($B(C_6F_5)_3$), leads to small differences in the NN distance, which are a little longer (**10**, 1.334(4), and **11**, 1.342(2) Å vs **9**[CHB$_{11}$H$_5$Br$_6$], 1.309(3), and **9**[B(C$_6$F$_5$)$_4$], 1.309(2) Å), while the CN bond lengths are identical to those in **9**[CHB$_{11}$H$_5$Br$_6$] and **9**[B(C$_6$F$_5$)$_4$]) (Figure 4, Table 3). The donor−acceptor bond lengths are in the expected range, at 1.480(4) (C1−C8) and 1.615(2) (C1−B1), respectively ($\sum r_{cov}$(C−C) = 1.50 Å and $\sum r_{cov}$(C−B) = 1.60 Å).[45]

*Pyrazole Species **7** and **12***. Both pyrazole species crystallize in the triclinic space group $P\bar{1}$ with two molecules per unit cell. As illustrated in Figure 5, the major difference in the molecular structure of both species arises from an intramolecular hydrogen bond in **12**, which forces a change of the configuration along the diazenyl substituent (cf. **7**, N4 trans to C3 vs **12**, N4 cis to C3), allowing the formation of a six-membered ring closed by the H-bridge. Furthermore, due to the hydrogen bond, the amino nitrogen atom of the $(Me_3Si)_2N$ moiety pyramidalizes ($\sum\angle$N = 338.1°) since the nitrogen lone pair cannot be delocalized by hyperconjugation. Hyperconjugative effects are known to be responsible for the planarization of the amino nitrogen atom, as found in **7**.[47] Both N atoms of the hydrazine substituent in **12** have a distorted trigonal-planar geometry ($\sum\angle$N = 359.4 and 359.7°), and both trigonal planes are almost perpendicular to each other (∠Si4−N5−N6−Si6 = 93.8°). Both (amino)silyl groups adopt a staggered configuration in contrast to **12**, for which an eclipsed configuration is observed. While the N5−N6 bond

dx.doi.org/10.1021/ja308104k | J. Am. Chem. Soc. 2012, 134, 17757−17768

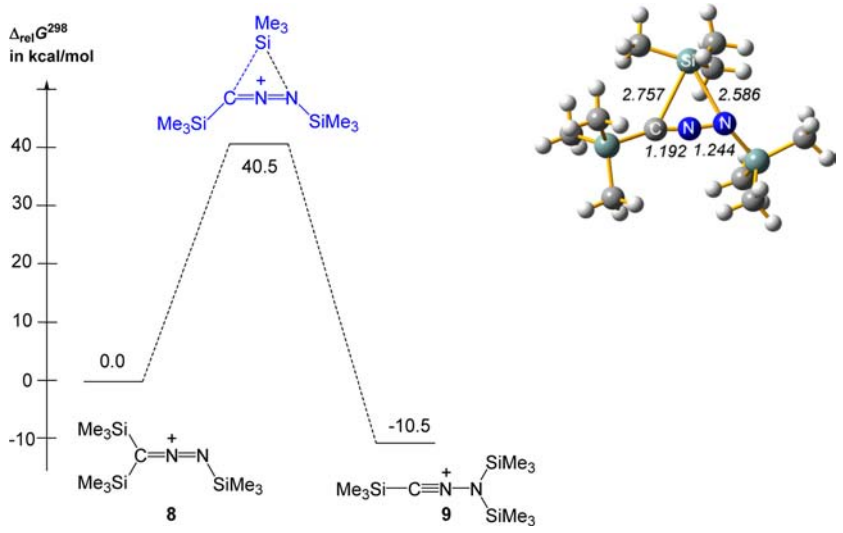

Figure 7. Left: Energies of the intrinsic isomerization process with a $[Me_3Si]^+$ ion as catalyst. Right: Calculated transition state for the intrinsic 1,3-Me_3Si shift in **8** (distances in Å).

lengths are similar in **7** (1.455(2) Å) and **12** (1.467(3) Å), the N3−N4 bond length of the diazenyl unit increases upon hydrogen bond formation in **12** (cf. 1.272(2) vs 1.348(3) Å; $\sum r_{cov}$(N═N) = 1.20 Å, $\sum r_{cov}$(N−N) = 1.42 Å;[45] 1.247(3) Å in Ph−N═N−Ph).[48] The central five-membered pyrazole ring is planar (deviation from planarity less than 2°), with bond lengths and angles in the expected ranges.[49]

2.4. Theoretical Aspects of the Trimerization Process. The astonishing isolation of $[(Me_3Si)_2NNC(SiMe_3)]^+$ instead of isomeric $[(Me_3Si)_2CNN(SiMe_3)]^+$ as well as the isolation of the trimerization product **7** prompted us to carry out quantum chemical calculations at the pbe1pbe/aug-cc-pwCVDZ level of theory to gain insight into the thermodynamics and kinetics of this complex reaction. In any case, the formation of pyrazole species **7**, starting from diazomethane, includes several successive reaction steps, including (i) a C−C or C−N coupling and (ii) a [3+2] or [4+1] cycloaddition reaction. Experimentally, it is known that pure $(Me_3Si)_2CNN$ is thermally stable for a long time. However, it is rearranged to bis(trimethylsilyl)carbodiimide, $(Me_3Si)NCN(SiMe_3)$, when it is heated in the presence of suitable catalysts such as Cu^{2+}.[33,41a] Thus, we studied the potential energy surface of neutral $(Me_3Si)_2CNN$ and cationic $[(Me_3Si)_3CNN]^+$ species, always retaining the CNN unit. As depicted in Scheme 5, the diazomethane isomer **1** is favored by 5.0 and 5.1 kcal/mol over nitrilimine **2** and aminoisonitrile **3**, respectively (cf. (Me_3Si)-$NCN(SiMe_3)$ lies 42.1 kcal/mol below **1**). Upon $[Me_3Si]^+$ addition this situation switches. Now isomer **9** generated from **2** and **3** represents the lowest-lying isomer, separated by 10.5 kcal/mol from cation **8**, in accord with the experimental observation (cf. $[(Me_3Si)_2NCN(SiMe_3)]^+$ lies 49.7 kcal/mol below **9**).

Two questions were addressed with respect to our experimental findings: (i) Why does diazomethane **1** isomerize to isonitrile **3** (which then trimerizes) upon addition of traces of $[Me_3Si]^+$, and (ii) why is cation **9** exclusively formed from diazomethane species **1** upon adding stoichiometric amounts of $[Me_3Si]^+$? To answer these questions we have calculated the transition states for the instrinsic 1,3-shift of a Me_3Si group in the neutral species **1** (Figure 6) and the cationic species **8** (Figure 7). In accord with our experimental data, the intrinsic isomerization process in neutral **1** at ambient temperatures is rather unlikely, since activation barriers larger than 56 kcal/mol need to be overcome. These barriers for a 1,3-shift considerably decrease once the $[Me_3Si]^+$ ion is added. However, they are still too large (ca. 40.5 kcal/mol, Figure 7) to allow such an intrinsic process at ambient or even low temperatures. Therefore, it can be assumed that bimolecular processes such as illustrated in Scheme 7 have to be considered. For the equilibrium of the

Scheme 7. Isomerization Equilibria of Bis-silylated Diazomethane Catalyzed by Silylium Ions

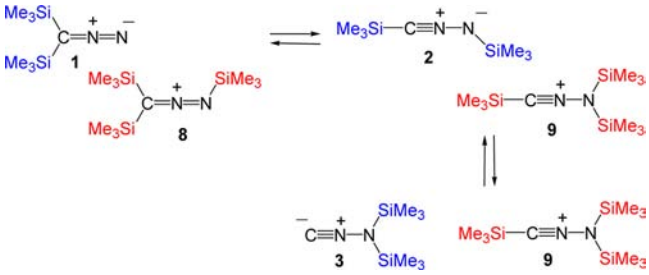

isomerization process, which includes both the neutral and the cationic species as catalyst according to Scheme 7, the ΔG^{298} values are estimated to be −5.5 and 0.1 kcal/mol, respectively, displaying $[Me_3Si]^+$ exchange equilibria. The barriers for $[Me_3Si]^+$ exchange are dramatically decreased under solvation conditions, as can be seen by studying the bimolecular reaction paths (Scheme 7). Now, the exchange of a $[Me_3Si]^+$ ion between cations **8** or **9** and the neutral isomers **1**, **2**, and **3** occurs almost barrier-free (less than 10 kcal/mol, see Supporting Information) at ambient temperatures, resulting in monosolvate formation of the type $[Me_3Si]^+ \cdot 2S$ adduct (S = **1**, **2**, and **3**). In the cases of **1** and **3**, these solvate adducts feature a trigonal planar $[Me_3Si]^+$ ion that is almost symmetrically stabilized by two S donor molecules (Figure 8). From these computational data, which are in agreement with experimental data, it can be concluded that the initial reaction step for the trimerization is the catalytic isomerization of diazomethane **1** and the cation **8** in a bimolecular process, as

dx.doi.org/10.1021/ja308104k | J. Am. Chem. Soc. 2012, 134, 17757−17768

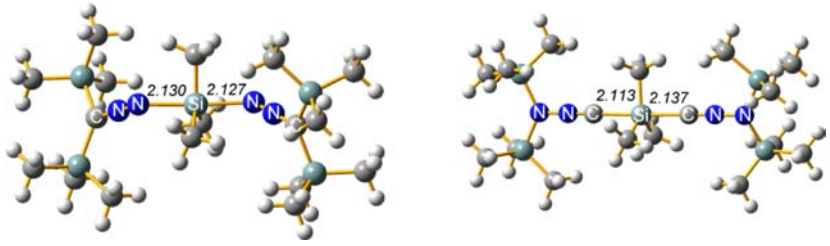

Figure 8. Calculated structures of stable $[Me_3Si]^+ \cdot 2S$ adducts: left, S = $(Me_3Si)_2CNN$ (**1**); right, S = $(Me_3Si)_2NNC$ (**3**). Distances in Å.

shown in Scheme 7, generating the reactive species **2** and **3**, respectively, besides cation **9**.

The trimethylsilylium affinity, which describes the enthalpy change associated with the dissociation of the conjugated acid,[50] is largest for isomer **2** (71.1 kcal/mol), followed by **3** (69.0 kcal/mol) and **1** (53.1 kcal/mol) (cf. Me_3Si−H, 31.3; Me_3Si−CN, 54.4; and $(Me_3Si)NCN(SiMe_3)$ 71.7 kcal/mol),[19] indicating that $[(Me_3Si)_2NNC(SiMe_3)]^+$ (**9**) is the most stable ion in the reaction mixture, in accord with experiment. Once the isomerization is triggered by the action of $[(Me_3Si)_2NNC(SiMe_3)]^+$, probably a dimerization via C−C or N−C coupling reaction of aminoisonitrile **3** occurs prior to a formal [3+2] or even [4+1] cycloaddition, as illustrated in Scheme 8. It is also possible that species **2** and **3** undergo dimerization. Since aminoisonitrile **3** is thermally stable in pure state and reacts only when the catalyst **9** is present, it can be concluded that also the dimerization reaction is catalyzed by strong Lewis acids (e.g., silylium ions $[(Me_3Si)_2NNC(SiMe_3)]^+$ + $(Me_3Si)_2NNC$). All three reactions steps are accompanied by formal Me_3Si shifts, which can easily occur upon addition of Me_3Si^+ ions (vide supra). Interestingly, according to *in situ* NMR experiments (see above), there is no experimental proof for the generation of a dimer or any other species involved in the proposed formal [3+2] or [4+1] cycloaddition. The fact that only pyrazole species **7** is observed besides the starting material indicates either a fast reaction on the NMR time scale or a very low concentration of the intermediates. The overall trimerization process according to Scheme 3 is exothermic/exergonic, with −67.0/−35.1 kcal/mol in the gas phase.

Scheme 8. Retrosynthetic Analysis of 7: (i) C−C Coupling Prior to [3+2] Cycloaddition, (ii) C−C Coupling Prior to [4+1] Cycloaddition, and (iii) C−N Coupling Prior to [4+1] Cycloaddition

2.5. Conclusions. We present an efficient and facile trimerization reaction of bis-silylated diazomethane, triggered by the action of silylium ions to give exclusively 4-diazenyl-3-hydrazinylpyrazole. As catalyst the isonitrilium ion $[(Me_3Si)_2NNC(SiMe_3)]^+$, a formal pseudo-chalcogonium ion, was identified and fully characterized for the first time. The reaction is described by an isomerization process followed by a C−C or N−C coupling reaction and a formal cycloaddition to give finally the pyrazole derivative. From a mechanistic viewpoint, we report the first trimerization of diazomethane derivatives, which could also be extended to the aminoisonitrile isomer. This transformation can be regarded as a domino reaction.[51] From a practical viewpoint, the chemistry reported herein provides a facile approach to novel hydrazine-diazene-substituted pyrazoles that are of pharmacological relevance and not readily available by other methods.[52,53]

3. EXPERIMENTAL DETAILS

3.1. General Information. All manipulations were carried out under oxygen- and moisture-free conditions under argon using standard Schlenk or drybox techniques.

Toluene and diethyl ether were dried over Na/benzophenone. *n*-Hexane and *n*-pentane were dried over Na/benzophenone/tetraglyme. Carbon tetrachloride, dichloromethane, and hexamethyldisiloxane $(Me_3Si)_2O$ were dried over P_4O_{10}. Acetone was dried by distillation from K_2CO_3 followed by storage over 3 Å molecular sieves for 24 h. All solvents were freshly distilled prior to use. *n*-Heptane, chlorotrimethylsilane Me_3SiCl (98%, Merck), and *N*,*N*-bis-(trimethylsilyl)carbodiimide $(Me_3Si)NCN(SiMe_3)$ (97%, abcr) were freshly distilled prior to use. Lithium (99.9%, Merck), gallium trichloride $GaCl_3$ (abcr, 99.9%), chloromethyltrimethylsilane Me_3SiCH_2Cl (97%, abcr), *n*-BuLi (2.5 M, Acros), and magnesium sulfate $MgSO_4$ (98%, VWR) were used as received. Alumina (aluminum oxide, basic, type T, Merck), was activated with triethylamine (98%, Merck) and dried in an oven at 120 °C for 36 h. *p*-Toluenesulfonylazide $MePhSO_2N_3$,[54] bis(trimethylsilyl)-hydronium tetrakis(pentafluorophenyl)borate $[Me_3Si{-}H{-}SiMe_3][B(C_6F_5)_4]$,[8b,15,55] tris(pentafluorophenyl)borane $B(C_6F_5)_3$,[55] tri-(phenyl)methylium tetrakis(pentafluorophenyl)borate $[Ph_3C][B(C_6F_5)_4]$,[55] trimethylsilyl(diethyl)oxonium tetrakis(pentafluoro-phenyl)borate $[Me_3SiOEt_2][B(C_6F_5)]$,[20,56] silver *closo*-7,8,9,10,11,12-hexabromocarboranate $Ag[CHB_{11}H_5Br_6]$,[57] trimethylsilylium *closo*-7,8,9,10,11,12-hexabromocarboranate $[Me_3Si][CHB_{11}H_5Br_6]$,[57] and bis(diethyloxo)hydronium tetrakis(pentafluorophenyl)borate $[(Et_2O)_2H][B(C_6F_5)_4]$[58] were prepared as previously reported. Trimethylsilyldiazomethane $Me_3SiCHNN$, bis(trimethylsilyl)-diazomethane $(Me_3Si)_2CNN$, *N*,*N*-bis(trimethylsilyl)aminoisonitrile dichloride $(Me_3Si)_2NNCCl_2$, and *N*,*N*-bis(trimethylsilyl)-aminoisonitrile $(Me_3Si)_2NNC$ have been reported in the literature and were prepared by slightly modified procedures.[33,34,59]

NMR. ^{29}Si INEPT, $^{13}C\{^1H\}$, ^{13}C DEPT, and ^1H NMR spectra were obtained on a Bruker AVANCE 250 or 300 spectrometer and were referenced internally to the deuterated solvent (^{13}C: $CDCl_3$, $\delta_{reference}$ = 77 ppm, CD_2Cl_2, $\delta_{reference}$ = 54 ppm, C_6D_6, $\delta_{reference}$ = 128 ppm) or to protic impurities in the deuterated solvent (^1H: $CHCl_3$, $\delta_{reference}$ = 7.26 ppm, $CDHCl_2$, $\delta_{reference}$ = 5.31 ppm, C_6D_5H, $\delta_{reference}$ = 7.16 ppm). $CDCl_3$ and CD_2Cl_2 were dried over P_4O_{10}; C_6D_6 was dried over Na/benzophenone and freshly distilled prior to use.

IR. A Nicolet 6700 FT-IR spectrometer with a Smart Endurance ATR device was used.

Raman. A Bruker VERTEX 70 FT-IR spectrometer with a RAM II FT-Raman module, equipped with a Nd:YAG laser (1064 nm), was used.

CHN Analyses. A C/H/N/S-Mikronalysator TruSpec-932 instrument from Leco was used.

dx.doi.org/10.1021/ja308104k | J. Am. Chem. Soc. 2012, 134, 17757−17768

DSC. A DSC 823e instrument from Mettler-Toledo (heating rate, 5 °C/min) was used. Melting points (and decomposition points) were corrected. In addition, clearing points are given in brackets.

MS. A Finnigan MAT 95-XP spectrometer from Thermo Electron was used (CI^+, isobutene; EI^+, T = 200 °C, 70.0 V).

HRMS. A 6210 time-of-flight LC/MS instrument from Agilent Technologies (MeOH/0.1% HCOOH in H_2O 90:10) was used.

3.2. Synthesis of 6[B(C$_6$F$_5$)$_4$]. To a stirred suspension of [Me_3Si−H−$SiMe_3$][$B(C_6F_5)_4$] (0.1 mmol, 0.083 g) in toluene (0.5 mL) was added neat (Me_3Si)NCN($SiMe_3$) (0.1 mmol, 0.019 g) at ambient temperature. The resulting colorless solution was concentrated *in vacuo*, resulting in a colorless oil. Storage at −25 °C for 24 h led to the deposition of colorless crystals. Removal of supernatant by decantation and drying *in vacuo* yields 0.072 g (0.077 mmol, 77%) of **6**[$B(C_6F_5)_4$]. Mp: 104 °C (106 °C). Anal. Calcd (found): C, 43.51 (43.52); H, 2.90 (2.98); N, 2.98 (2.95). IR (ATR, 16 scans): 3467 (w), 3408 (w), 3381 (w), 3327 (w), 2962 (w), 2912 (w), 2359 (w), 2320 (m), 2287 (w), 2243 (m), 1643 (m), 1558 (w), 1512 (s), 1456 (s), 1412 (m), 1383 (m), 1374 (m), 1317 (m), 1263 (s), 974 (s), 907 (m), 853 (s), 823 (s), 768 (s), 755 (s), 726 (m), 700 (w), 683 (m), 661 (s), 634 (m), 610 (m), 603 (m), 573 (m). Raman (190 mW, 25 °C, 400 scans, cm^{-1}): 2982 (4), 2973 (4), 2913 (10), 2251 (4), 1648 (4), 1516 (1), 1468 (1), 1422 (1), 1380 (2), 1322 (2), 1277 (1), 1266 (1), 1127 (1), 1110 (1), 1098 (1), 1088 (1), 1056 (1), 980 (1), 824 (3), 774 (2), 760 (1), 710 (1), 687 (1), 664 (1), 645 (8), 587 (6), 531 (1), 494 (5), 479 (5), 452 (6), 425 (5), 398 (5), 381 (1), 361 (1), 350 (1), 290 (1), 248 (2), 210 (1), 190 (2), 161 (1), 124 (1), 76 (1). MS (CI^+, isobutane): 259 [$(SiMe_3)_3CN_2]^+$, 187 [$(SiMe_3)_2CN_2 + H]^+$, 115 [$(SiMe_3)CN_2$ + $2H]^+$. Crystals suitable for X-ray crystallographic analysis were obtained from slowly cooling a saturated toluene solution of **6**[$B(C_6F_5)_4$] to 5 °C over a period of 12 h.

3.3. Synthesis of 9[B(C$_6$F$_5$)$_4$] and Catalytic Reaction to 7. *Procedure 1: Reaction with (Me_3Si)$_2$CNN.* To a stirred suspension of [Me_3Si−H−$SiMe_3$][$B(C_6F_5)_4$] (0.05 mmol, 0.040 g) in *n*-pentane (2 mL) was added a solution of $(Me_3Si)_2CNN$ (1.06 mmol, 0.197 g) in *n*-pentane (2 mL) at −78 °C. The resulting suspension was allowed to warm to ambient temperature. Stirring for 36 h resulted in the deposition of crystals while the color of the supernatant changed gradually from yellow to dark red. The supernatant was removed by filtration (F4), and the brownish residue was washed three times with *n*-pentane (3 mL). Recrystallization from a minimum of toluene at −25 °C resulted in the deposition of colorless crystals. Removal of supernatant by decantation and drying *in vacuo* yielded 0.022 g (0.02 mmol, 49% yield based on 0.05 mmol of [Me_3Si−H−$SiMe_3$][$B(C_6F_5)_4$]) of **9**[$B(C_6F_5)_4$] as colorless crystals. The solutions from filtration and washing were combined, and the solvent was removed *in vacuo*, resulting in a dark red solution. Storage at −25 °C led to the deposition of greenish crystals. Removal of supernatant and drying *in vacuo* yielded 0.097 g (0.17 mmol, 51%) of **7** as dark green crystals.

Procedure 2: Reaction with (Me_3Si)$_2$NNC. To a stirred suspension of [Me_3Si−H−$SiMe_3$][$B(C_6F_5)_4$] (0.05 mmol, 0.041 g) in *n*-hexane (4 mL) was added neat $(Me_3Si)_2NNC$ (1.0 mmol, 0.186 g) at −78 °C. The resulting suspension was allowed to warm slowly to ambient temperature. Stirring for 12 h resulted in the deposition of yellowish crystals while the color of the supernatant changed gradually from yellow to dark red. The supernatant was removed by filtration (F4), and the yellowish residue was washed with *n*-hexane (3 mL). Recrystallization from a minimum of toluene at 5 °C resulted in the deposition of colorless crystals. Removal of supernatant by decantation and drying *in vacuo* yielded 0.027 g (0.03 mmol, 58% yield based on 0.05 mmol [Me_3Si−H−$SiMe_3$][$B(C_6F_5)_4$]) of **9**[$B(C_6F_5)_4$] as colorless crystals. The solutions from filtration and washing were combined and concentrated *in vacuo*, resulting in a dark red solution. Storage at −25 °C led to the deposition of greenish crystals. Removal of supernatant and drying *in vacuo* yielded 0.120 g (0.21 mmol, 68%) of **7** as dark green crystals.

*Data for **9**[B(C$_6$F$_5$)$_4$]*. Mp: 108 °C (109 °C). Anal. Calcd (found): C, 43.51 (43.75); H, 2.90 (2.85); N, 2.98 (2.86). IR (ATR, 16 scans): 3374 (w), 3224 (w), 2962 (w), 2912 (w), 2327 (w), 2215 (m), 1643 (m), 1600 (w), 1556 (w), 1512 (s), 1460 (s), 1413 (m), 1382 (m), 1374 (m), 1340 (w), 1261 (m), 1167 (m), 1081 (s), 976 (s), 923 (w), 907 (w), 855 (s), 822 (s), 773 (m), 768 (m), 756 (s), 726 (m), 700 (w), 683 (m), 660 (m), 643 (m) 626 (m), 611 (m), 602 (m), 573 (m). Raman (1500 mW, 25 °C, 800 scans, cm^{-1}): 2970 (4), 2910 (10), 2209 (9), 1643 (3), 1598 (1), 1576 (1), 1536 (1), 1513 (1), 1454 (1), 1417 (1), 1375 (2), 1314 (1), 1276 (1), 1263 (1), 1125 (1), 1106 (1), 976 (1), 960 (1), 945 (1), 862 (1), 845 (1), 820 (3), 771 (1), 757 (1), 733 (1), 700 (1), 685 (1), 661 (1), 643 (5), 628 (5), 584 (7), 509 (2), 491 (5), 476 (4), 448 (6), 422 (4), 394 (5), 371 (1), 359 (1), 348 (1), 320 (1), 287 (1), 265 (1), 244 (1), 206 (1), 186 (2), 157 (1), 119 (1). MS (CI^+, isobutane): 259 [$(SiMe_3)_3CN_2]^+$, 187 [$(SiMe_3)_2CN_2 + H]^+$. Crystals suitable for X-ray crystallographic analysis were obtained from toluene as depicted above.

*Data for **7***. Mp: 66 °C (70 °C). Anal. Calcd (found): C, 45.10 (45.15); H, 9.73 (9.44); N, 15.03 (15.05). ^{1}H NMR (25 °C, CD_2Cl_2, 300.13 MHz): 0.15 (s, 18H, $Si(CH_3)_3$), 0.16 (s, 9H, $Si(CH_3)_3$), 0.28 (s, 9H, $Si(CH_3)_3$), 0.32 (s, 9H, $Si(CH_3)_3$), 0.48 (s, 9H, $Si(CH_3)_3$). ^{1}H NMR (25 °C, C_6D_6, 300.13 MHz): 0.23 (s, 9H, $Si(CH_3)_3$), 0.35 (s, 18H, $Si(CH_3)_3$), 0.37 (s, 9H, $Si(CH_3)_3$), 0.44(s, 9H, $Si(CH_3)_3$), 0.48(s, 9H, $Si(CH_3)_3$). $^{13}C\{^1H\}$ NMR (25 °C, CD_2Cl_2, 62.89 MHz): −3.35 (s, $Si(CH_3)_3$), −0.21 (s, $Si(CH_3)_3$), 0.08 (s, $(Si(CH_3)_3)_2$), 0.11 (s, $Si(CH_3)_3$), 0.29 (s, $Si(CH_3)_3$), 137.29 (*C*), 146.91(*C*), 158.15 (*C*). $^{13}C\{^1H\}$ NMR (25 °C, C_6D_6, 62.89 MHz): −0.64 (s, $Si(CH_3)_3$), 2.58 (s, $Si(CH_3)_3$), 2.75 (s, $Si(CH_3)_3$), 3.02 (s, 2 $Si(CH_3)_3$), 140.26 (*C*), 149.72 (*C*), 161.15 (*C*). $^{29}Si\{^1H\}$ NMR (25 °C, CD_2Cl_2, 49.69 MHz): −13.39 (m, 1Si, $J(^1H-^{29}Si)$ = 6.82 Hz), 6.22 (m, 1Si, $J(^1H-^{29}Si)$ = 6.79 Hz), 8.94 (m, 2Si, $J(^1H-^{29}Si)$ = 6.65 Hz), 11.31 (m, 1Si, $J(^1H-^{29}Si)$ = 6.59 Hz), 17.15 (m,1Si, $J(^1H-^{29}Si)$ = 6.71 Hz). $^{29}Si\{^1H\}$ NMR (25 °C, C_6D_6, 49.69 MHz): −13.71 (m, 1Si, $J(^1H-^{29}Si)$ = 6.54 Hz), 6.00 (m, 1Si, $J(^1H-^{29}Si)$ = 6.54 Hz), 9.09 (m, 2Si, $J(^1H-^{29}Si)$ = 6.54 Hz), 11.40 (m, 1Si, $J(^1H-^{29}Si)$ = 6.54 Hz), 17.17 (m, 1Si, $J(^1H-^{29}Si)$ = 6.54 Hz). IR (ATR, 16 scans): 2956 (m), 2899 (m), 2864 (w), 1603 (w), 1574 (w), 1565 (w), 1521 (w), 1510 (w), 1490 (m), 1454 (m), 1388 (m), 1363 (m), 1298 (w), 1279 (m), 1245 (s), 1178 (m), 1142 (w), 1103 (w), 1074 (m), 1022 (w), 1004 (w), 981(w), 939 (m), 875 (m), 832 (s), 822 (s), 753 (s), 726 (m), 890 (m), 632 (m), 621 (m), 561 (w), 532 (m). Raman (1500 mW, 25 °C, 1209 scans, cm^{-1}): 2957 (3), 2903 (10), 1490 (2), 1453 (2), 1388 (7), 1364 (9), 1282 (5), 1245 (1), 1103 (1), 1080 (1), 1006 (1), 964 (2), 946 (1), 878 (1), 838 (1), 748 (1), 726 (1), 693 (3), 610 (3), 535 (1), 472 (1), 454 (1), 407 (1), 376 (1), 351 (1), 340 (1), 308 (1), 256 (1), 204 (1), 182 (1), 114 (1). MS (CI^+, isobutane): 558 $[M]^+$, 543 $[M - CH_3]^+$, 486 $[M - SiMe_3]^+$. UV−vis (25 °C, CH_2Cl_2, nm): 556, 393, 321, 255. Crystals suitable for X-ray crystallographic analysis were obtained by slowly cooling a saturated solution of **7** in either *n*-pentane, *n*-hexane, hexamethyldisiloxane, or acetone to −25 °C over a period of up to 12 h. Crystals obtained from *n*-hexane and hexamethyldisiloxane solutions could be characterized as *n*-hexane hemisolvate (**7**·*n*-hexane) or hexamethyldisiloxane hemisolvate (**7**·disiloxane), while crystals from *n*-pentane or acetone solutions did not contain solvent. However, the *n*-hexane was easily removed upon drying at ambient temperature for a few minutes.

3.4. Synthesis of 9[CHB$_{11}$H$_5$Br$_6$]. To a stirred brownish suspension of [Me_3Si][$CHB_{11}H_5Br_6$] (0.1 mmol, 0.069 g) in toluene (3.0 mL) was added neat $(Me_3Si)_2NNC$ (0.6 mmol, 0.120 g) at ambient temperature. The resulting colorless suspension was allowed to stir for an additional 1 h. Removal of supernatant by syringe and drying *in vacuo* yielded 0.068 g (0.0785 mmol, 79%) of **9**[$CHB_{11}H_5Br_6$] as pale brownish microcrystalline solid. Mp (dec): 206 °C. Anal. Calcd (found): C, 15.08 (14.88); H, 3.80 (4.06); N, 3.20 (3.50). ^{1}H NMR (25 °C, CD_2Cl_2, 300.13 MHz): 0.47 (s, 18H, $J(^1H-^{29}Si)$ = 6.6 Hz, $J(^1H-^{13}C)$ = 121 Hz), 0.64 (s, 9H, $J(^1H-^{29}Si)$ = 7.18 Hz, $J(^1H-^{13}C)$ = 124 Hz), 1.12−3.57 (m, 5H, B*H*, $J(^1H-^{11}B)$ = 159 Hz), 2.59 (s, 1H, *CH-carboranate*). ^{11}B NMR (25 °C, CD_2Cl_2, 96.29 MHz) −20.22 (d, 5B, *B*H), −9.84 (s, 5B, *B*Br), −1.74 (s, 1B, 12-BBr). $^{13}C\{^1H\}$ NMR (25 °C, CD_2Cl_2, 75.48 MHz): −1.32 (s, $Si(CH_3)_3$), −0.15 (s, 2$Si(CH_3)_3$). $^{29}Si\{^1H\}$ NMR (25 °C, CD_2Cl_2, 59.62 MHz): 4.78 (1*Si*), 29.01 (2*Si*). IR (ATR, 16 scans): 3051 (w), 2958 (w), 2902 (w), 2606 (m), 2236 (w), 2165 (w), 1682 (w), 1417 (w), 1309 (w), 1256 (s), 1113 (m), 1054 (m), 1002 (m), 991 (m),

dx.doi.org/10.1021/ja308104k | J. Am. Chem. Soc. 2012, 134, 17757−17768

953 (m), 933 (m), 855 (s), 819 (s), 746 (s), 702 (m), 633 (s). MS (CI−, isobutane): 616 *m/e* $[CHB_{11}H_5Br_6]^-$. Crystals suitable for X-ray crystallographic analysis of **9**$[CHB_{11}H_5Br_6]$ were obtained from the saturated catalyst phase of the benzene reaction mixture after 12 h.

3.5. Synthesis of $[(Me_3Si)_2NNC(CPh_3)]B(C_6F_5)_4]$ (10). To a stirred orange solution of $[Ph_3C][B(C_6F_5)_4]$ (0.5 mmol, 0.427 g) in dichloromethane (3 mL) was added neat $(Me_3Si)_2NNC$ (0.5 mmol, 0.093 g) at ambient temperature. The mixture was allowed to stir for 1 h while the color of the solution changed within 20 min from orange to yellow. Slow addition of *n*-hexane (5 mL) resulted in the deposition of a yellow greenish, microcrystalline solid. The yellow supernatant was removed by syringe, and the residue was re-dissolved in dichloromethane (2 mL) and again precipitated by addition of *n*-hexane (4 mL). This procedure was repeated a further two times. Removal of supernatant by decantation and drying *in vacuo* yielded 0.324 g (0.29 mmol, 58%) of $[(Me_3Si)_2NNC(CPh_3)]B(C_6F_5)_4]$ as microcrystalline solid. Mp (dec): 136 °C. Anal. Calcd (found): C, 54.16 (54.03); H, 3.00 (3.09); N, 2.53 (2.62). ^{1}H NMR (25 °C, CD_2Cl_2, 300.13 MHz): 0.38 (s, 18H, $J(^1H-^{29}Si)$ = 6.8 Hz, $J(^1H-^{13}C)$ = 121 Hz), 7.08−7.53 (m, 15H, C*H*). $^{19}F\{^1H\}$ NMR (25 °C, CD_2Cl_2, 282.4 MHz): δ = −167.5 (m, *m*-C*F*), −163.6 (m, *p*-C*F*), −133.0 (m, *o*-C*F*). ^{11}B NMR (25 °C, CD_2Cl_2, 96.29 MHz) −16.64. $^{13}C\{^1H\}$ NMR (25 °C, CD_2Cl_2, 75.48 MHz): 0.10 (s, $Si(CH_3)_3$), 124.59 (br, *ipso*-C), 129.11 (s, *C*H), 130.43 (s, *C*H), 130.75 (s, *p*-CH), 136.91 (dm, *m*-CF, $^1J(^{13}C-^{19}F)$ = 247.59 Hz), 138.90 (dm, *p*-CF, $^1J(^{13}C-^{19}F)$ = 232.18 Hz), 148.76 (dm, *o*-CF, $^1J(^{13}C-^{19}F)$ = 240.44 Hz). $^{29}Si\{^1H\}$ NMR (25 °C, CD_2Cl_2, 59.62 MHz): 30.87. IR (ATR, 16 scans): 2959 (w), 2913 (w), 2285 (w), 1643 (m), 1599 (w), 1584 (w), 1512 (s), 1493 (w), 1460 (s), 1456 (s), 1411 (m), 1383 (w), 1373 (w), 1359 (w), 1265 (m), 1186 (w), 1171 (w), 1160 (w), 1145 (w), 1084 (s), 1033 (w), 1001 (w), 974 (s), 942 (m), 902 (m), 854 (s), 823 (s), 773 (m), 756 (s), 748 (s), 726 (m), 698 (s), 683 (s), 660 (s), 635 (m), 610 (m), 603 (m), 573 (m). MS (CI+, isobutane): 431 (40) [M + H], 521 (10) $[B(C_6F_5)_3]$, 357 (10) $[Me_3SiN(H)NCCPh_3]$, 167 (78) $[C_6F_5]$, 187 (10) $[(SiMe_3)_2NNC + H]$, 270 (38) $[Ph_3CCN + H]$. Crystals suitable for X-ray crystallographic analysis were obtained from slow diffusion of *n*-hexane onto the saturated dichloromethane solution of **10** at ambient temperature over a period of 36 h.

3.6. Synthesis of $(Me_3Si)_2NNC(B(C_6F_5)_3)$ (11). *Procedure 1: Reaction with $(Me_3Si)_2NNC$.* To a stirred solution of $B(C_6F_5)_3$ (0.5 mmol, 0.256 g) in dichloromethane (2.5 mL) neat $(Me_3Si)_2NNC$ (0.5 mmol, 0.094 g) was added at 0 °C. The stirred reaction mixture was allowed to warm to ambient temperature within 1 h. The pale yellow solution was filtered (F4), concentrated approximately to 0.7 mL and stored in the refrigerator (5 °C) for 12 h. The resulting colorless Crystals were washed with dichloromethane (0.5 mL). Removal of supernatant by syringe and drying *in vacuo* yielded 0.250 g (0.358 mmol, 72%) of $(Me_3Si)_2NNC(B(C_6F_5)_3)$ (**11**).

Procedure 2: Reaction with $(Me_3Si)_2CNN$. To a stirred solution of $B(C_6F_5)_3$ (0.5 mmol, 0.256 g) in dichloromethane (2.5 mL) was added neat $(Me_3Si)_2CNN$ (0.6 mmol, 0.120 g) at 0 °C. The stirred reaction mixture was allowed to warm to ambient temperature within 1 h. The pale yellow solution was filtered (F4), concentrated approximately to 0.7 mL, and stored in the refrigerator (5 °C) for 12 h. The resulting colorless crystals were washed with dichloromethane (0.5 mL). Removal of supernatant by syringe and drying *in vacuo* yielded 0.178 g (0.255 mmol, 51%) of $(Me_3Si)_2NNCB(C_6F_5)_3$ (**11**).

*Data for **11**.* Mp: 122 °C (124 °C). Anal. Calcd (found): C, 42.99 (43.04); H, 2.60 (2.84); N, 4.01 (3.75). ^{1}H NMR (25 °C, CD_2Cl_2, 300.13 MHz): 0.29 (s, 18H, $J(^1H-^{29}Si)$ = 6.8 Hz, $J(^1H-^{13}C)$ = 121 Hz). $^{19}F\{^1H\}$ NMR (25 °C, CD_2Cl_2, 282.4 MHz): δ = −164.5 (m, *m*-C*F*), −157.9 (m, *p*-C*F*), −133.4 (m, *o*-C*F*). ^{11}B NMR (25 °C, CD_2Cl_2, 96.29 MHz): −21.27. $^{13}C\{^1H\}$ NMR (25 °C, CD_2Cl_2, 75.48 MHz): −0.36 (s, $Si(CH_3)_3$), 116.02 (br, *ipso*-C), 137.63 (dm, *m*-CF, $^1J(^{13}C-^{19}F)$ = 229.43 Hz), 140.77 (dm, *p*-CF, $^1J(^{13}C-^{19}F)$ = 214.03 Hz), 148.58 (dm, *o*-CF, $^1J(^{13}C-^{19}F)$ = 240.99 Hz). $^{29}Si\{^1H\}$ NMR (25 °C, CD_2Cl_2, 59.62 MHz): 25.46. IR (ATR, 16 scans): 2972 (w), 2911 (w), 2302 (w), 1645 (m), 1557 (w), 1514 (s), 1470 (s), 1466 (s), 1456 (s), 1418 (m), 1392 (m), 1382 (s), 1287 (m), 1282 (m), 1261 (s), 1134 (m), 1127 (m), 1095 (s), 1029 (w), 979 (s), 968 (s), 928 (w), 890 (m), 880 (m), 854 (s), 826 (s), 800 (s), 764 (m), 747 (m), 728 (m), 700 (m), 680 (m), 672 (m), 647 (m), 630 (m), 577 (w). Raman (460 mW, 25 °C, 200 scans, cm^{-1}): 2974 (5), 2913 (10), 2797 (4), 2539 (3), 2299 (10), 2220 (3), 1650 (4), 1474 (1), 1422 (1), 1394 (2), 1279 (2), 1138 (1), 1098 (1), 861 (1), 803 (2), 766 (1), 753 (1), 710 (1), 685 (1), 676 (1), 652 (6),635 (1), 622 (1), 585 (10), 510 (2), 496 (4), 471 (8), 450 (7), 419 (4), 398 (6), 357 (1), 344 (1), 288 (1), 271 (1), 244 (2), 188 (2), 159 (2), 91 (3). MS (EI, 70 eV): 698 (10) [M], 531 (14) $[M - C_6F_5]$, 512 (100) $[B(C_6F_5)_3]$, 364 (13) $[M - 2C_6F_5]$, 186 (11) $[(SiMe_3)_2NNC]$, 73 (83) $[(SiMe_3)]$. Crystals suitable for X-ray crystallographic analysis were obtained by slowly cooling a saturated dichloromethane solution of **11** to 5 °C over a period of 12 h.

3.7. Synthesis of 12. *Procedure 1.* To a stirred solution of **7** (0.48 mmol, 0.271 g) in *n*-hexane (5 mL) was added neat CF_3SO_3H (0.50 mmol, 0.075 g) dropwise at ambient temperature with stirring. The resulting suspension was stirred for 2 h while the color of the supernatant changed gradually from brown red to yellowish orange, and the yellowish precipitate was dissolved completely. Concentration to an approximate volume of 0.5 mL and storage at 5 °C resulted in the deposition of yellow crystals. Removal of supernatant, washing with a few drops of *n*-hexane, and drying *in vacuo* yielded 0.140 g (59%) of **12** as yellow crystals.

Procedure 2. **7** (0.179 mmol, 0.1 g) was dissolved in distilled (but not anhydrous) *n*-hexane (3 mL) at ambient temperature with stirring. The resulting orange solution was stirred for 15 min. Concentration to an approximate volume of 0.5 mL and storage at 5 °C resulted in the deposition of yellowish crystals. Removal of supernatant and drying *in vacuo* yielded 0.085 g (97%) of **12** as yellow crystals.

*Data for **12**.* Mp: 94 °C (101 °C). Anal. Calcd (found): C, 44.39 (44.57); H, 9.523 (9.33); N, 17.26 (17.25). ^{1}H NMR (25 °C, C_6D_6, 500.13 MHz): 10.15 (s, 1H, N*H*), 0.52 (s, 9H, $Si(CH_3)_3$, N-1), 0.41 (s, 9H, $Si(CH_3)_3$, C-1), 0.27 (s, 9H, $Si(CH_3)_3$, N-4), 0.15 (s, 18H, 2 $Si(CH_3)_3$, N-6). $^{13}C\{^1H\}$ NMR (25 °C, C_6D_6, 128.0 MHz): 161.9, 142.1 (*C*-2, *C*-3), 157.3 (*C*-1), 0.3 (s, 2 $Si(CH_3)_3$, N-6), −0.5 (s, $Si(CH_3)_3$, N-1), −0.6 (s, $Si(CH_3)_3$, N-4), −1.5 (s, $Si(CH_3)_3$, *C*-1). $^{29}Si\{^1H\}$ NMR (25 °C, C_6D_6, TMS = 0, 99.3 MHz): 10.1, 7.4 ($SiMe_3$(N-1), $SiMe_3$(N-4)), 6.6 (2, $SiMe_3$(N-6)), −8.6 ($SiMe_3$(C-1)). ^{1}H NMR (25 °C, CD_2Cl_2, 300.13 MHz): 0.10 (s, 18H, $N(Si(CH_3)_3)_2$, $J(^1H-^{29}Si)$ = 6.6 Hz), 0.24 (s, 9H, $Si(CH_3)_3$, $J(^1H-^{29}Si)$ = 6.9 Hz, $J(^1H-^{13}C)$ = 121 Hz), 0.29 (s, 9H, $Si(CH_3)_3$), 0.37 (s, 9H, $Si(CH_3)_3$, $J(^1H-^{29}Si)$ = 6.9 Hz, $J(^1H-^{13}C)$ = 120 Hz), 9.97 (s, 1H, N*H*). $^{13}C\{^1H\}$ NMR (25 °C, CD_2Cl_2, 62.89 MHz): −1.36 (s, $Si(CH_3)_3$), −0.32 (s, $Si(CH_3)_3$), −0.21 (s, $Si(CH_3)_3$), 0.56 (s, $(Si(CH_3)_3)_2$), 141.9 (*C*), 157.7 (*C*), 161.9 (*C*). $^{29}Si\{^1H\}$ NMR (25 °C, CD_2Cl_2, 99.3 MHz): −8.79, 6.91, 7.91, 9.91. IR (ATR, 16 scans): 2956 (m), 2899 (m), 2855 (w), 1573 (m), 1563 (m), 1520 (m), 1465 (m), 1405 (m), 1345 (w), 1325 (w), 1300 (m), 1245 (s), 1179 (s), 1076 (m), 1050 (m), 982 (m), 961 (m), 930 (m), 898 (m), 870 (m), 828 (s), 818 (s), 753 (s), 693 (m), 662 (m), 628 (s), 601 (m). Raman (1500 mW, 25 °C, 800 scans, cm^{-1}): 2960 (5), 2900 (10), 1562 (1), 1522 (1), 1466 (4), 1411 (1), 1345 (1), 1300 (1), 1250 (1), 1179 (1), 1076 (1), 983 (1), 963 (1), 941 (1), 898 (1), 843 (1), 763 (1), 694 (1), 663 (1), 634 (2), 601 (1), 531 (1), 462 (1), 435 (1), 357 (1), 318 (1), 303 (1), 235 (1), 177 (1), 117 (1). MS (CI^+, isobutane): 486 $[M]^+$, 471 $[M - CH_3]^+$, 413 $[M - SiMe_3]^+$. UV−vis (25 °C, CH_2Cl_2, nm): 412, 294.

■ ASSOCIATED CONTENT

Supporting Information

Experimental and computational details, crystallographic information, and further experimental and theoretical data of all considered species. This material is available free of charge via the Internet at http://pubs.acs.org.

■ AUTHOR INFORMATION

Corresponding Author

axel.schulz@uni-rostock.de

Notes

The authors declare no competing financial interest.

■ ACKNOWLEDGMENTS

Martin Ruhmann (University Rostock) is acknowledged for the measurement of Raman spectra. Financial support by the DFG is gratefully acknowledged.

■ REFERENCES

(1) (a) Lambert, J. B.; Zhao, Y. *Angew. Chem., Int. Ed. Engl.* **1997**, *36*, 400−402. (b) Lambert, J. B.; Zhao, Y.; Wu, H.; Tse, W. C.; Kuhlmann, B. *J. Am. Chem. Soc.* **1999**, *121*, 5001−5008. (c) Lambert, J. B.; Lin, L. *J. Org. Chem.* **2001**, *66*, 8537−8539.

(2) Reviews: (a) Schulz, A.; Villinger, A. *Angew. Chem., Int. Ed.* **2012**, *51*, 4526−4528. (b) Lee, V. Y.; Sekiguchi, A. *Organometallic Compounds of Low-Coordinate Si, Ge, Sn and Pb*; Wiley: Chichester, 2010. (c) Klare, H. F. T.; Oestreich, M. *Dalton Trans.* **2010**, *39*, 9176−9184. (d) Lee, V. Y.; Sekiguchi, A. In *Reviews of Reactive Intermediate Chemistry*; Platz, M. S., Moss, R. A., Jones, M., Eds.; Wiley: New York, 2007; pp 47−120. (e) Lee, V. Y.; Sekiguchi, A. *Acc. Chem. Res.* **2007**, *40*, 410−419. (f) Müller, T. *Adv. Organomet. Chem.* **2005**, *53*, 155−215. (g) Kochina, T. A.; Vrazhnov, D. V.; Sinotova, E. N.; Voronkov, M. G. *Russ. Chem. Rev.* **2006**, *75*, 95−110. (h) Lambert, J. B.; Zhao, Y.; Zhang, S. M. *J. Phys. Org. Chem.* **2001**, *14*, 370−379. (i) Reed, C. A. *Acc. Chem. Res.* **1998**, *31*, 325−332. (j) Lickiss, P. D. In *The Chemistry of Organic Silicon Compounds*; Rappoport, Z., Apeloig, Y., Eds.; Wiley: Chichester, 1998; Vol. 2, pp 557−594. (k) Lambert, J. B.; Kania, L.; Zhang, S. *Chem. Rev.* **1995**, *95*, 1191−1201.

(3) For example: (a) Schäfer, A.; Reißmann, M.; Schäfer, A.; Saak, W.; Haase, D.; Müller, T. *Angew. Chem., Int. Ed.* **2011**, *50*, 12636−12638. (b) Allemann, O.; Duttwyler, S.; Romanato, P.; Baldrige, K. K.; Siegel, J. S. *Science* **2011**, *332*, 574−577. (c) Müther, K.; Fröhlich, R.; Mück-Lichtenfeld, C.; Grimme, S.; Oestreich, M. *J. Am. Chem. Soc.* **2011**, *133*, 12442−12444. (d) Müther, K.; Oestreich, M. *Chem. Commun.* **2011**, *47*, 334−336. (e) Leszczyńska, K.; Mix, A.; Berger, R. J. F.; Rummel, B.; Neumann, B.; Stammler, H.-G.; Jutzi, P. *Angew. Chem., Int. Ed.* **2011**, *50*, 6843−6846. (f) Duttwyler, S.; Douvris, C.; Nathanael, C. D.; Fackler, N. L.; Tham, F. S.; Reed, C. A.; Baldrige, K. K.; Siegel, J. S. *Angew. Chem., Int. Ed.* **2010**, *49*, 7519−7522. (g) Lühmann, N.; Panisch, R.; Müller, T. *Appl. Organomet. Chem.* **2010**, *24*, 533−537. (h) Klare, H. F. T.; Bergander, K.; Oestreich, M. *Angew. Chem., Int. Ed.* **2009**, *48*, 9077−9079. (i) Douvris, C.; Ozerov, O. *Science* **2008**, *321*, 1188−1190. (j) Panisch, R.; Boldte, M.; Müller, T. *J. Am. Chem. Soc.* **2006**, *128*, 9676−9682. (k) Hara, K.; Akiyama, R.; Sawamura, M. *Org. Lett.* **2005**, *7*, 5621−5623.

(4) Scott, V. J.; Çelenligil-Çetin, R.; Ozerov, O. V. *J. Am. Chem. Soc.* **2005**, *127*, 2852−2853.

(5) Meier, G.; Braun, T. *Angew. Chem., Int. Ed.* **2009**, *48*, 1546−1548.

(6) Zhang, Y.; Huynh, K.; Manners, I.; Reed, C. A. *Chem. Commun.* **2008**, 494−496.

(7) In contrast, siliconium ions are positively charged species in which silicon has higher than four coordination. Some authors prefer to restrict the term silylium ion to the fully tricoordinate form. See also: http://old.iupac.org/publications/books/rbook/Red_Book_2005.pdf.

(8) (a) Lambert, J. B.; Zhang, S.; Stern, C. L.; Huffman, J. C. *Science* **1993**, *260*, 1917−1918. (b) Lambert, J. B.; Zhang, S.; Ciro, S. M. *Organometallics* **1994**, *13*, 2430−2443.

(9) Xie, Z.; Liston, D. J.; Jelinek, T.; Mitro, V.; Bau, R.; Reed, C. A. *J. Chem. Soc., Chem. Commun.* **1993**, 384−386.

(10) Ibad, M. F.; Langer, P.; Schulz, A.; Villinger, A. *J. Am. Chem. Soc.* **2011**, *133*, 21016−21027.

(11) Duttwyler, S.; Do, Q.-Q.; Linden, A.; Baldridge, K. K.; Siegel, J. S. *Angew. Chem., Int. Ed.* **2008**, *47*, 1719−1722.

(12) Müller, T.; Bauch, C.; Ostermeier, M.; Bolte, M.; Auner, N. *J. Am. Chem. Soc.* **2003**, *125*, 2158−2168.

(13) Maerker, C.; Kapp, J.; Schleyer, P. von, R. In *Organosilicon Chemistry II*; Auner, N., Weis, J., Eds.; VCH: Weinheim, Germany, 1996; pp 329−358.

(14) Kim, K.-C.; Reed, C. A.; Elliott, D. W.; Mueller, L. J.; Tham, F.; Lin, L.; Lambert, J. B. *Science* **2002**, *297*, 825−827.

(15) Lehmann, M.; Schulz, A.; Villinger, A. *Angew. Chem., Int. Ed.* **2009**, *48*, 7444−7447.

(16) Lambert, J. B.; Zhang, S. *J. Chem. Soc., Chem. Commun.* **1993**, 383−384.

(17) Reed, C. A.; Xie, Z.; Bau, R.; Benesi, A. *Science* **1993**, *262*, 402−404.

(18) (a) Prakash, G. K. S.; Keyaniyan, S.; Aniszfeld, R.; Heiliger, L.; Olah, G. A.; Stevens, R. C.; Choi, H.-K.; Bau, R. *J. Am. Chem. Soc.* **1987**, *109*, 5123−5126. (b) Lambert, J. B.; Schulz, W. J., jr.; McConnell, J. A.; Schilf, W. *J. Am. Chem. Soc.* **1988**, *110*, 2201−2210.

(19) Schulz, A.; Villinger, A. *Chem.—Eur. J.* **2010**, *16*, 7276−7281.

(20) Schulz, A.; Thomas, J.; Villinger, A. *Chem. Commun.* **2010**, *46*, 3696−3698.

(21) Jäger, L.; Köhler, H. *Sulfur Rep.* **1992**, *12*, 159−212.

(22) Huisgen, R. In *1,3-Dipolar Cycloaddition Chemistry*; Padwa, A., Ed.; Wiley: New York, 1984; pp 1−31.

(23) (a) Regitz, M. *Diazoalkane: Eigenschaften und Synthesen*; Thieme Verlag: Stuttgart, 1977. (b) Zollinger, H. *Diazo Chemistry I*; VCH: Weinheim, 1994. (c) Zollinger, H. In *Diazo Chemistry II*; VCH: Weinheim, 1995. (d) Ye, T.; McKervey, M. A. *Chem. Rev.* **1994**, *94*, 1091−1160.

(24) (a) Fink, J.; Regitz, M. *Synthesis* **1985**, 569−585. (b) Bug, T.; Hartnagel, M.; Schlierf, C.; Mayr, H. *Chem.—Eur. J.* **2003**, *9*, 4068−4076.

(25) Huisgen, R. *Angew. Chem.* **1955**, *67*, 439−461.

(26) (a) Ledwith, A.; Shih-Lin, Y. *J. Chem. Soc. B* **1967**, 83−84. (b) Huisgen, R. *Angew. Chem., Int. Ed. Engl.* **1963**, *2*, 565−598. (c) Huisgen, R. *Angew. Chem., Int. Ed. Engl.* **1963**, *2*, 633−696.

(27) (a) Fustero, S.; Sánchez-Roselló, M.; Barrio, P.; Simón-Fuentes, A. *Chem. Rev.* **2011**, *111*, 6984−7034. (b) Elguero, J.; Silva, A. M. S.; Tome, A. C. In *Modern Heterocyclic Chemistry*, Vol. 2; Alvarez-Builla, J., Vaquero, J. J., Barluenga, J., Eds.; Wiley-VCH: Weinheim, 2011; pp 635−725.

(28) (a) Metwally, M. A.; Darwish, Y. M.; Amer, F. A. *Indian J. Chem., Sect. B* **1989**, *28*, 1069−1071. (b) Zauhar, L. *Can. J. Chem.* **1968**, *46*, 1079−1085. (c) Karci, F.; Sener, N.; Yamac, M.; Sener, I.; Demircali, A. *Dyes Pigm.* **2008**, *80*, 47−52. (d) Fahmy, S. H.; El-Hosami, M.; El-Gamal, S.; Elnagdi, M. H. *J. Chem. Technol. Biotechnol.* **1982**, *32*, 1042−1048.

(29) Mohareb, R. M.; Ho, J. Z.; Alfarouk, F. O. *J. Chin. Chem. Soc.* **2007**, *54*, 1053−1066.

(30) (a) Boger, D. L.; Coleman, R. S.; Panek, J. S.; Huber, F. X.; Sauer, J. *J. Org. Chem.* **1985**, *50*, 5377−5379. (b) Boger, D. L.; Panek, J. S.; Duff, S. R. *J. Am. Chem. Soc.* **1985**, *107*, 5745−5754. (c) Sotiropoulos, J. M.; Baceiredo, A.; Bertrand, G. *Bull. Soc. Chim. Fr.* **1992**, *129*, 367−375.

(31) (a) Meerwein, H. *Angew. Chem.* **1948**, *60*, 78. (b) Kantor, S. W.; Osthoff, R. C. *J. Am. Chem. Soc.* **1953**, *75*, 931−932.

(32) Only one major resonance Lewis formula is shown for clarity.

(33) Seyferth, D.; Flood, T. C. *J. Organomet. Chem.* **1971**, *29*, C25−C28.

(34) Wiberg, N.; Hübler, G. *Z. Naturforsch.* **1976**, *31b*, 1317−1321.

(35) (a) Huisgen, R.; Seidel, M.; Sauer, J.; McFarland, J. W.; Wallbillich, G. *J. Org. Chem.* **1959**, *24*, 892−893. (b) Huisgen, R.; Seidel, M.; Wallbillich, G.; Knupfer, H. *Tetrahedron* **1962**, *17*, 3−29.

(36) Bertrand, G.; Wentrup, C. *Angew. Chem., Int. Ed. Engl.* **1994**, *33*, 527−545.

(37) Granier, M.; Baceiredo, A.; Dartiguenave, Y.; Dartiguenave, M.; Menu, M. J.; Bertrand, G. *J. Am. Chem. Soc.* **1990**, *112*, 6277−6285.

(38) Emig, N.; Gabbaï, F. P.; Krautscheid, H.; Réau, R.; Bertrand, G. *Angew. Chem., Int. Ed.* **1998**, *37*, 989−992.

(39) Castan, F.; Baceiredo, A.; Bertrand, G. *Angew. Chem., Int. Ed.* **1989**, 1250−1251.

(40) (a) Pump, J.; Wannagat, U. *Liebigs Ann.* **1962**, *652*, 21−27. (b) Stenzel, J.; Sundermeyer, W. *Chem. Ber.* **1967**, *100*, 3368−3370. (c) Drake, J. E.; Glavincevski, B. M.; Henderson, H. E.; Wong, C. *Can. J. Chem.* **1979**, *57*, 1162−1166. (d) Kienzle, A.; Obermeyer, A.; Riedel, R.; Aldinger, F.; Simon, A. *Chem. Ber.* **1993**, *126*, 2569−2571.
(41) (a) Seyferth, D.; Menzel, H.; Dow, A. W.; Flood, T. C. *J. Organomet. Chem.* **1972**, *44*, 279−290. (b) Seyferth, D.; Dow, A. W.; Menzel, H.; Flood, T. C. *J. Am. Chem. Soc.* **1968**, *90*, 1080−1082.
(42) Jacobsen, H.; Berke, H.; Doering, S.; Kehr, G.; Erker, G.; Froehlich, R.; Meyer, O. *Organometallics* **1999**, *18*, 1724−1735.
(43) Addition of an excess of CF_3SO_3H leads to a complete Me_3Si/H substitution of all N-bound Me_3Si groups. Only the C-bound $SiMe_3$ group remains intact.
(44) Obermeyer, A.; Kienzle, A.; Weidlein, J.; Riedel, R.; Simon, A. *Z. Anorg. Allg. Chem.* **1994**, *620*, 1357−1363.
(45) Pyykkö, P.; Atsumi, M. *Chem.—Eur. J.* **2009**, *15*, 12770−12779.
(46) (a) Glendening, E. D.; Reed, A. E.; Carpenter, J. E.; Weinhold, F. *NBO*, Version 3.1. (b) Carpenter, J. E.; Weinhold, F. *J. Mol. Struct. (Theochem)* **1988**, *169*, 41−62. (c) Weinhold, F.; Carpenter, J. E. *The Structure of Small Molecules and Ions*; Plenum Press: New York, 1988; p 227. (d) Weinhold, F.; Landis, C. *Valency and Bonding. A Natural Bond Orbital Donor-Acceptor Perspective*; Cambridge University Press: Cambridge, UK, 2005; and references therein.
(47) Fischer, G.; Herler, S.; Mayer, P.; Schulz, A.; Villinger, A.; Weigand, J. J. *Inorg. Chem.* **2005**, *44*, 1740−1751.
(48) Brown, C. J. *Acta Crystallogr.* **1966**, *21*, 146.
(49) Prasad, T. N. M.; Raghava, B.; Sridhar, M. A.; Rangappa, K. S.; Prasad, J. S. *X-ray Struct. Anal. Online* **2010**, *26*, 75.
(50) Swart, M.; Rösler, E.; Bickelhaupt, M. *J. Comput. Chem.* **2006**, 1485−1492.
(51) Reviews: (a) Tietze, L. F.; Beifuss, U. *Angew. Chem., Int. Ed. Engl.* **1993**, *32*, 131−163. (b) Tietze, L. F. *Chem. Rev.* **1996**, *96*, 115−136.
(52) (a) Musad, E. A.; Lokanatha, R. K. M.; Mohamed, R.; Saeed, A. B.; Vishwanath, B. S.; Rao, K. M. L. *Bioorg. Med. Chem. Lett.* **2011**, *21*, 3536−3540. (b) Kaymakcioglu, B. K.; Rollas, S. *Farmaco* **2002**, *57*, 595−600. (c) Coumar, M. S.; Leou, J.-S.; Shukla, P.; Wu, J.-S.; Dixit, A. K.; Lin, W.-H.; Chang, C.-Y.; Lien, T.-W.; Chen, C.-H.; Hsu, J. T.-A; Chao, Y.-S.; Wu, S.-Y.; Hsieh, H.-P.; Tan, U.-K., Jr. *J. Med. Chem.* **2009**, *52*, 1050−1062. (d) Ali, T. E.; Abdel-Aziz, S. A.; El-Shaaer, H. M.; Hanafy, F. I.; El-Fauomy, A. Z. *Phosphorus, Sulfur, Silicon Relat. Elem.* **2008**, *183*, 2139−2160. (e) Silveira, I. A. F. B.; Paulo, L. C.; de Miranda, A. L. P.; Rocha, S. O.; Freitas, A. C. C.; Barreiro, E. J. *J. Pharm. Pharmacol.* **1993**, *45*, 646−649.
(53) (a) El-Shafei, A.; Fadda, A. A.; Khalil, A. M.; Ameen, T. A. E.; Badria, F. A. *Bioorg. Med. Chem.* **2009**, *17*, 5096−5105. (b) El-Hawash, S. A.; Habib, N. S.; Fanaki, N. H. *Pharmazie* **1999**, *54*, 808−813. (c) Khalil, Z. H.; Yanni, A. S.; Gaber, A. M.; Abdel-Mohsen, S. A. *Phosphorus, Sulfur, Silicon Relat. Elem.* **2000**, *166*, 57−70. (d) Bekhit, A. A.; Ashour, H. M. A.; Guemei, A. A. *Arch. Pharm.* **2005**, *338*, 167−174. (e) Amir, M.; Khan, S. A.; Drabu, S. *J. Indian Chem. Soc.* **2002**, *79*, 280−281. (f) Krystof, V.; Cankar, P.; Frysova, I.; Slouka, J.; Kontopidis, G.; Dzubak, P.; Hajduch, M.; Srovnal, J.; de Azevedo, W. F.; Orsag, M.; Paprskarova, M.; Rolccik, J.; Latr, A.; Fischer, P. M.; Strnad, M. *J. Med. Chem.* **2006**, *49*, 6500−6509.
(54) Reiß, F.; Schulz, A.; Villinger, A.; Weding, N. *Dalton. Trans.* **2010**, *39*, 9962−9972.
(55) Nava, M.; Reed, C. A. *Organometallics* **2011**, *30*, 4798−4800.
(56) Driess, M.; Barmeyer, R.; Monsé, C.; Merz, K. *Angew. Chem., Int. Ed.* **2001**, *40*, 2308−2310.
(57) (a) Dunks, G. B.; Palmer-Ordonez, K. *Inorg. Chem.* **1978**, *17*, 1514−1516. (b) Dunks, G. B.; Barker, K.; Hedaya, E.; Hefner, C.; Palmer-Ordonez, K.; Remec, P. *Inorg. Chem.* **1981**, *20*, 1692−1697. (c) Franken, A.; King, B. T.; Rudolph, J.; Rao, P.; Noll, B. C.; Michl, J. *Collect. Czech. Chem. Commun.* **2001**, *66*, 1238−1249. (d) Xie, Z.; Jelinek, T.; Bau, R.; Reed, C. A. *J. Am. Chem. Soc.* **1994**, *116*, 1907−1913. (e) Xie, Z.; Bau, R.; Benesi, A.; Reed, C. *Organometallics* **1995**, *14*, 3933−3941.
(58) (a) Reiß, F.; Schulz, A.; Villinger, A. *Eur. J. Inorg. Chem.* **2012**, 261−271. (b) Jutzi, P.; Müller, C.; Stammler, A.; Stammler, H.-G. *Organometallics* **2000**, *19*, 1442−1444.
(59) Barton, T. J.; Hoekman, S. K. *Synth. React. Inorg. Met.-Org. Chem.* **1979**, *9*, 297−300.